# *Streptococcus agalactiae* MprF synthesizes a novel cationic glycolipid that promotes brain entry and meningitis

Luke R. Joyce[1], Haider S. Manzer[2], Jéssica da C. Mendonça[2], Ricardo Villarreal[2], Kelly S. Doran[2#], Kelli L. Palmer[1#], and Ziqiang Guan[3#]

[1]Department of Biological Sciences, The University of Texas at Dallas, Richardson, TX, USA

[2]Department of Immunology and Microbiology, University of Colorado School of Medicine, Aurora, CO, USA

[3]Department of Biochemistry, Duke University Medical Center, Durham, NC, USA

**Running title:** GBS lysine lipids contribute to meningitis

#Corresponding authors

Kelly S. Doran: Kelly.Doran@CUAnschutz.edu

Kelli L. Palmer: Kelli.Palmer@UTDallas.edu

Ziqiang Guan: Ziqiang.Guan@Duke.edu

**Conflict of interest**

The authors have declared that no conflict of interest exists.

**Abstract**

*Streptococcus agalactiae* (Group B *Streptococcus*; GBS) is the etiological agent of meningitis and severe invasive diseases in newborns. The cellular membrane, a critical site for host-pathogen interactions, is poorly characterized in GBS. Here, we analyzed the GBS lipidome using liquid chromatography coupled with electrospray ionization tandem mass spectrometry. We identified a novel amino-acylated glycolipid, lysyl-glucosyl-diacylglycerol (Lys-Glc-DAG), which is abundant in all GBS strains analyzed. Through heterologous expression and gene deletion, we demonstrate that the GBS multiple peptide resistance factor (MprF) synthesizes Lys-Glc-DAG, as well as lysyl-phosphatidylglycerol (Lys-PG), which has been characterized in many pathogenic bacteria. Consistent with a critical role in host-GBS interactions, the GBS∆*mprF* mutant exhibited a reduction of surface net negative charge and a significantly reduced ability to invade human cerebral microvascular endothelial cells. Further, mice challenged with the GBS∆*mprF* mutant developed bacteremia comparably to wild-type GBS-challenged mice, yet exhibited fewer bacterial counts in the brain and less meningeal inflammation. Overall, we demonstrate that GBS has uniquely evolved a multifunctional MprF enzyme that results in the synthesis of a major cationic membrane glycolipid and plays a significant role in meningitis pathogenesis. Moreover, our results illustrate the novel insights obtained from comprehensive lipidomic profiling of major human pathogens.

## Introduction

*Streptococcus agalactiae* (Group B *Streptococcus*; GBS) is a Gram-positive, β-hemolytic bacterium that colonizes the lower genital and gastrointestinal tracts of approximately 30% of healthy women (1,2). GBS causes disease in healthy adults and pregnant woman and opportunistically causes life-threatening neonatal infections such as meningitis, sepsis, and pneumonia (3–7). GBS can be transmitted from colonized mothers to newborns during natural childbirth, and due to the severity of the resulting diseases, intrapartum antibiotic prophylaxis is prescribed for colonized pregnant women (8,9). Even with these measures, the GBS is still a leading cause of neonatal meningitis that results in long-lasting neurological effects in surviving infants (4–7).

Research on the pathogenesis of the GBS has mainly focused on cell wall-anchored or secreted proteins and polysaccharides that aid in the attachment to and invasion of host cells. The numerous attachment and virulence factors possessed by the GBS are summarized in a recent review by Armistead *et al* 2019 (10). Comparatively little is known about GBS cellular membrane lipids, even though the bacterial membrane is a critical site for host-pathogen interactions. To our knowledge, the only characterization of GBS phospholipids prior to our current study was the identification of the phospholipids phosphatidylglycerol (PG), cardiolipin (CL), and lysyl-phosphatidylglycerol (Lys-PG) in GBS (11,12). Similarly, investigation into the glycolipids of the GBS membrane has focused on di-glucosyl-diacylglycerol ($Glc_2$-DAG), which is the lipid anchor of the Type I lipoteichoic acid, and its role in pathogenesis (13).

Previous genomic analyses of GBS have identified a homolog of MprF (multiple peptide resistance factor) (14), an enzyme which catalyzes the aminoacylation of the anionic phospholipid PG in a range of Gram-positive and Gram-negative bacteria (15,16). MprF is a membrane-bound enzyme comprised of a N-terminal flippase domain (17) and a C-terminal catalytic domain that catalyzes the aminoacylation of the glycerol group of PG by using aminoacyl-tRNAs as the amino acid donors (18,19). An important function of aminoacylation, in particular lysylation, of PG in the membranes of bacteria is to lower the net negative charge of their cellular envelope to protect them from cationic antimicrobial peptides (CAMPs) produced by host immune systems and bacteriocins produced by competitor bacteria (15,16).

In this study, we utilized normal phase liquid chromatography (NPLC) coupled with electrospray ionization (ESI) high-resolution tandem mass spectrometry (HRMS/MS) to characterize the GBS membrane lipid composition, and identified a novel cationic glycolipid, lysyl-glucosyl-diacylglycerol (Lys-Glc-DAG), which comprises a major portion of the GBS total lipid extract. While Lys-PG has been reported in a range of bacterial species (20), Lys-Glc-DAG represents, to our knowledge, the first example of lysine modification of a neutral glycolipid. By gene deletion and heterologous expression, we show the GBS MprF enzyme is responsible for the biosynthesis of both the novel Lys-Glc-DAG and Lys-PG. We hypothesize that this expanded substrate repertoire of MprF allows for more extensive masking of the negative charges of the cellular membrane, contributing to GBS pathogenesis.

## Results

### Identification of Lys-Glc-DAG, a novel cationic glycolipid in GBS

To characterize the membrane lipids of GBS cultured in Todd-Hewitt Broth (THB), three clinical isolates of representative serotypes were used: COH1 (serotype III) (21) , A909 (serotype Ia) (22), and CNCTC 10/84 (serotype V) (23,24). Lipid extraction was performed using an acidic Bligh-Dyer method (25–27), followed by lipidomic analysis by normal phase LC-ESI/MS performed in both positive and negative ion modes. Figure 1A shows the total ion chromatogram (TIC) of LC-ESI/MS of the lipid extract of COH1 in the negative mode. Common Gram-positive bacterial lipids were identified by negative ion ESI/MS/MS, including diacylglyercol (DAG), monohexosyldiacylglycerol (MHDAG), dihexosyldiacylglycerol (DHDAG), PG, lyso-phosphatidylglycerol (lyso-PG), CL, Lys-PG, phosphatidic acid (PA), and undecaprenyl phosphate ($C_{55}$-P) (Table 1).

Surprisingly, the positive TIC (Figure 1B) shows highly abundant peaks of unknown identity at the retention time ~25-29 min. These TIC peaks are derived from *m/z* 803.595, *m/z* 831.624, *m/z* 857.644, *m/z* 885.671 and *m/z* 913.703 ions (Figure 1C), which are indicative of a lipid with varying acyl chain lengths. These ions were interpreted as $[M+H]^+$, given their corresponding $[M-H]^-$ and $[M+Cl]^-$ ions were detected in the negative mode (not shown). The mass spectra and LC retention times of this unknown lipid do not match with any other bacterial lipids we have analyzed. Searching lipidomic databases by exact masses did not result in any matches. The unknown lipid was also observed in A909 and CNCTC 10/84 strains (Supplementary Figure 1). To identify this unknown lipid, MS/MS was performed in both positive and negative ion modes.

Positive ion MS/MS spectrum of *m/z* 885.6 (the most abundant species with a molecular mass of 884.6 Da) produced structurally informative fragments (Figure 1D). In particular, the low-mass fragments *m/z* 84.045 and *m/z* 129.061 are indicators of the presence of amino acids, with lysine being a strong possibility (28). The *m/z* 129 is proposed to be formed from lysine by elimination of $H_2O$; it fragments further to produce *m/z* 84, a low mass ion observed in the spectra of many lysine derivatives (28). The $NH_3$ loss peak observed at *m/z* 868.6 resulted from the elimination of an amino group of the lysine side chain. The accurate mass measurement of fragments indicates that lysine is linked to a hexose moiety. Specifically, the exact mass difference between *m/z* 291.114 and *m/z* 129.056 is 162.053, which is in agreement with the elemental composition of a hexose subunit ($C_6H_{10}O_5$, calculated mass 162.053). Negative ion MS/MS provided further structural information. As shown in Figure 1E, MS/MS of the $[M-H]^-$ ion at *m/z* 883.6 produced a major fragment ion at *m/z* 145.08, which corresponds to a deprotonated lysine. The *m/z* 255.2 and 281.2 ions are the carboxylic anions of palmitic (C16:0) and oleic (C18:1) fatty acids, respectively, revealing the two acyl chains of the most abundant molecular species (MW 884.6).

Based on the above MS/MS and exact mass measurement, we propose lysyl-glucosyl-diacylglyerol (Lys-Glc-DAG) (Figure 1F) as the structure of this unknown lipid. The assignment of glucose was based on the observation that glucosyl-diacylglycerol (Glc-DAG), the precursor of Lys-Glc-DAG, is a major membrane component of GBS and other streptococci (13,29), as well as the results from an isotopic labeling experiment using a

$^{13}C$-labeled glucose, described below. The chemical structure of Lys-Glc-DAG is consistent with its chromatographic properties under normal phase LC conditions. Due to the presence of both polar (glucose) and charged (lysine) groups which bind strongly with the silica-based stationary phase, Lys-Glc-DAG has longer retention times than other major lipids in GBS. Also, Lys-Glc-DAG consists of several molecular species with different fatty acyl compositions. These different Lys-Glc-DAG molecular species have slightly different retention times, giving rise to multiple, unresolved TIC peaks (~25-29 min). The observed and calculated exact masses of major Lys-Glc-DAG molecular ion species are shown in Table 2.

**Isotopic incorporation of lysine and glucose into Lys-Glc-DAG**

To further confirm the lysine and glucose moieties of Lys-Glc-DAG, we carried out stable isotope-labeling experiments by culturing COH1 in streptococcal defined media (DM) supplemented with either deuterated lysine or $^{13}C$-labeled glucose. In the deuterated lysine (lysine-*d4*), 4 hydrogen (1 Da) atoms across 2 of the carbon atoms are replaced with deuterium (2 Da) atoms, thereby increasing the mass of lysine by 4 Da. Figure 2A and 2B show the positive ion mass spectra of the $[M+H]^+$ ions of Lys-Glc-DAG species extracted from cultures in DM and in DM supplemented with lysine-*d4*, respectively. The incorporation of lysine-*d4* into Lys-Glc-DAG is reflected by a 4 Da mass shift between the $[M+H]^+$ ions of the unlabeled Lys-Glc-DAG (blue dots) and the lysine-*d4*-labeled Lys-Glc-DAG (red dots). The same 4 Da mass shift is observed in the negative ion mode: the $[M-H]^-$ ion of unlabeled Lys-Glc-DAG (16:0/18:1) is observed at *m/z* 883.6, while the lysine-*d4* containing Lys-Glc-DAG (16:0/18:1) is observed at *m/z* 887.6 (Supplementary Figure

2A). Furthermore, MS/MS of *m/z* 883.6 (Supplementary Figure 2B) and *m/z* 887.6 (Supplementary Figure 2C) produced fragment ions at *m/z* 145 and *m/z* 149, corresponding to the deprotonated lysine and lysine-*d4*, respectively. The molecular weight shift of lysine-*d4* incorporation is also observed in Lys-PG (Supplementary Figure 2D). The incorporation of lysine-*d4* is shown by a 4 Da mass shift between the $[M+H]^+$ ions of *m/z* 887.6 unlabeled Lys-PG (blue dots) to the *m/z* 881.6 lysine-*d4*-labeled Lys-PG (red dots).

In D-Glucose (U-$^{13}C_6$), all six carbon (12 Da) atoms are replaced with carbon-13 atoms ($^{13}C$), thereby increasing the mass of glucose by 6 Da. In contrast to lysine-*d4* labeling, the molecular profile of Lys-Glc-DAG from $^{13}C$-labeled glucose labeling is more complex. This is because $^{13}C$-labeled glucose is utilized by GBS not only to replace the glucose moiety of Lys-Glc-DAG, but also to synthesize its fatty acyl chains via glycolysis. As shown in Figure 2C, the *m/z* 885.6 $[M+H]^+$ ion of unlabeled Lys-Glc-DAG (16:0/18:1) is shifted to a broader distribution of ion peaks ranging from *m/z* 894.7 to 910.7. The mass shifts (numbers in red) indicate the numbers of total $^{13}C$ atoms being incorporated into the Lys-Glc-DAG (16:0/18:1) molecule. To locate the incorporated $^{13}C$ atoms on Lys-Glc-DAG, MS/MS was performed on one of the most abundant ion species. Supplementary Figure 2E shows the MS/MS spectrum of *m/z* 885.6 of Lys-Glc-DAG in THB and Supplementary Figure 2F shows the MS/MS spectrum of *m/z* 900.7 in DM supplemented with D-Glucose-$^{13}C_6$ (containing a total of fifteen $^{13}C$ atoms). The replacement of glucose by D-Glucose (U-$^{13}C_6$) in Lys-Glc-DAG is evidenced by a 6 Da mass shift of the lysyl-glucosyl moiety from *m/z* 291.1 (Supplementary Figure 2E) to *m/z* 297.1 (Supplementary

Figure 2F). The other nine $^{13}C$ atoms must be distributed in the diacylglycerol portion of Lys-Glc-DAG. Furthermore, careful comparison of both MS/MS spectra of labeled and unlabeled Lys-Glc-DAG indicates that the lysine residue is linked to the 6-position of glucose; the fragmentation schemes for *m/z* 189.0 (no $^{13}C$ atoms) (Supplementary Figure 2E) and $^{13}C$-labeled *m/z* 191.0 (two $^{13}C$ atoms) (Supplementary Figure 2F) are indicated.

**Heterologous expression of GBS *mprF* in *S. mitis* results in the production of both Lys-Glc-DAG and Lys-PG**

GBS encode an ortholog of MprF (14). MprF catalyzes the aminoacylation of PG to form Lys-PG and other minor aminoacyl-PGs such as Ala-PG and Arg-PG in other bacterial species (15,16). Our identification of Lys-PG in the cellular membrane of the GBS confirms that an active MprF is present in GBS.

To ascertain if the GBS MprF is responsible for the addition of lysine to Glc-DAG to form Lys-Glc-DAG, a heterologous host expression system was designed in *Streptococcus mitis* ATCC 49456, a *S. mitis* type strain. We selected *S. mitis* because it does not encode *mprF* and it is naturally transformable. Moreover, our previous lipidomic analysis confirmed that it does not synthesize Lys-PG, but does synthesize Glc-DAG, the precursor of Lys-Glc-DAG, as a major membrane component (27,30). The gene encoding GBS COH1 *mprF*, GBSCOH1_1931, was cloned into pABG5Δ*phoZ* (31) for expression (the empty vector is referred to as pABG5 hereafter). As controls, the two *mprF* genes of *Enterococcus faecium* strain 1,231,410, EFTG_00601 (*mprF1*) and EFTG_02430 (*mprF2*), were also cloned for expression in *S. mitis*. One *E. faecium mprF* allele (*mprF1*)

has been experimentally verified to direct synthesis of Lys-PG, while the second one (*mprF2*) does not (18).

*S. mitis* strains were cultured overnight in THB before lipidomics was performed. Figure 2A-C shows the lipidomic profile of *S. mitis* (pABG5) (empty vector control), *S. mitis* (pEfmMprF1), and *S. mitis* (pGBSMprF). In Figure 3, Panel 1 shows the TIC, Panel 2 shows the MS of the retention time 19.5 – 21.5 min expected for Lys-PG, and Panel 3 shows the MS of the retention time 26 – 30 min expected for Lys-Glc-DAG. Phosphatidylcholine, a previously described membrane lipid in *S. mitis* (27), elutes off the column at roughly the same time as Lys-PG. The empty vector control strain does not synthesize Lys-PG (Figure 3A, Panel 2) or Lys-Glc-DAG (Figure 3A, Panel 3). In *S. mitis* (pEfmMprF1), Lys-PG is observed in the membrane (Figure 3B, Panel 2) but no Lys-Glc-DAG is present (Figure 3B, Panel 3), which is consistent with previous findings in *E. faecium* (18). As expected, *S. mitis* (pEfmMprF2) does not produce Lys-PG (Supplementary Figure 3). Finally, *S. mitis* (pGBSMprF) synthesizes high levels of Lys-Glc-DAG, as shown by a large TIC peak at 26 to 30 min (Figure 3C, Panel 1). MS spectra indicate Lys-PG is present in the membrane (Figure 3C, Panel 2) and Lys-Glc-DAG is produced (Figure 3C, Panel 3) with major molecular species at *m/z* 857 and *m/z* 885, which are also detected in the GBS membrane. Taken together, these heterologous host expression results in *S. mitis* reveal that GBS MprF not only synthesizes Lys-PG but also possesses the unique and novel activity of modifying Glc-DAG to form Lys-Glc-DAG.

**Deletion of *mprF* in GBS results in the loss of synthesis of Lys-PG and Lys-Glc-DAG**

To validate the function of MprF in the synthesis of Lys-Glc-DAG *in vivo* in GBS, we deleted the *mprF* gene, GBSCOH1_1931, from the COH1 genome using the sucrose sensitivity selection plasmid pMBSacB (32) and confirmed the deletion by whole genome sequencing. Figure 4A Panel 1 shows COH1 wild-type (WT) TIC and the abundance of Lys-PG (Figure 4A, Panel 2) and Lys-Glc-DAG (Figure 4A, Panel 3). The COH1Δ*mprF* TIC shows a complete loss of Lys-PG and Lys-Glc-DAG (Figure 4B, Panel 1), supported by the absence of ions of Lys-PG (Figure 4B, Panel 2) and Lys-Glc-DAG (Figure 4B, Panel 3) in the corresponding ESI/MS spectra. The complemented strain, COH1Δ*mprF* (pGBSmprF), has a TIC lipid profile similar to that of WT COH1 (Figure 4C, Panel 1) and shows the resotration of both Lys-PG (Figure 4C, Panel 2) and Lys-Glc-DAG (Figure 4C, Panel 3). Together these data conclusively demonstrate that GBS MprF is responsible for synthesizing both Lys-PG and Lys-Glc-DAG. While MprF is well-known to modify anionic PG with lysine and other amino acids, to our knowledge aminoacylation of a neutral lipid has not been reported. Overall, these data conclusively demonstrate a novel function of GBS MprF (Figure 5). These results also demonstrate that, even though Lys-Glc-DAG makes up a relatively large proportion of the total lipid extract, it is non-essential for growth under the laboratory conditions tested here.

**GBS synthesize lysine lipids in various physiological lysine concentrations.**

GBS are lysine auxotrophs (33). In the human host, L-lysine has been quantified in varying concentrations throughout the body, from ~43 μM in cerebrospinal fluid to ~441

μM in blood (34). To confirm the production of Lys-PG and Lys-Glc-DAG under the physiological lysine concentrations, a lysine titration was performed in DM. At 50 μM lysine concentration, the GBS growth was reduced and reached an overnight $OD_{600nm}$ of ~0.36 (compare to normal overnight growth of ~$OD_{600nm}$ 1.75 with 600 μM lysine). Lys-PG and Lys-Glc-DAG were always present in the GBS membrane, but their levels varied in a lysine-dependent manner at concentrations ranging from 50 μM to 600 μM (Figure 6A and Supplementary Figure 4A-D). These data demonstrate considerable levels of Lys-PG and Lys-Glc-DAG are present in the GBS membrane, even in the lower range of physiological concentrations of lysine, which we expect to have physiological roles in the GBS membrane.

**A GBS *mprF* mutant has altered cell surface charge, pH stress survival, and cellular chain length**

Aminoacylated phospholipids, especially Lys-PG, reduce the negative charges on the outer surface of the membrane and aid in survival under acidic conditions in other bacteria (15,16,35,36). To investigate the effects of the lysine lipids on the GBS membrane surface charge, Cytochrome C binding assays were performed. Cytochrome C is positively charged, and more Cytochrome C bound to bacterial cells indicates a greater net negative outer surface charge. The Δ*mprF* mutant bound significantly more Cytochrome C compared to WT COH1 and complement strains (Figure 6B). To assess the ability of the Δ*mprF* mutant to survive in acidic conditions, a pH-adjusted growth assay was performed. The growth of the Δ*mprF* mutant was reduced at a pH of 5.5, and the mutant failed to grow at pH 5, compared to WT COH1 and complement strains (Figure 6C). Finally, given

the substantial membrane charge alteration in the Δ*mprF* mutant (Figure 6B), we assessed whether removal of the lysine lipids from the GBS membrane altered the cell morphology and/or division phenotype. Confocal microscopy with a membrane dye was performed on overnight cultures. It was observed that the Δ*mprF* mutant grew in significantly longer chains compared to WT COH1 (Figure 6D). Finally, the lysine lipids did not impact GBS hemolytic activity (Supplementary Figure 4E), and there was no difference in growth observed between COH1(pABG5), COH1Δ*mprF*(pABG5), and COH1Δ*mprF*(pGBSMprF) strains in THB medium *in vitro* (Supplementary Figure 4F). Taken together, these results indicate important and specific physiological roles for the lysine lipids in the membrane of the GBS.

**Lysine lipids are involved in GBS interactions with human cells *in vitro***

Next, we determined whether loss of Lys-PG and Lys-Glc-DAG altered host cell interaction. To mimic the human blood-brain barrier (BBB), the human cerebral microvascular endothelial cell line hCMEC/D3 was utilized. The *in vitro* assays for adhesion and invasion were performed using pre-established protocols (37,38). To control for the presence of the plasmid backbone in the complement strain, COH1(pABG5), COH1Δ*mprF*(pABG5), and COH1Δ*mprF*(pGBSMprF) strains were used. There was no significant difference in the number of Δ*mprF* mutant compared to WT and complement cells attached to hCMEC/D3 cells (Figure 7A). However, Figure 7B shows a significant decrease in the number of Δ*mprF* mutant cells able to invade the hCMEC/D3 cells. The human vaginal epithelial cell line VK2/E6E7 was also utilized for the same assays (Supplementary Figure 5). Interestingly, the Δ*mprF* mutant had a significant

decrease in the ability to both adhere and invade the VK2/E6E7 cell line (Supplementary Figure 5A and 5B). Taken together, these data indicate that lysine lipids influence the ability of GBS to invade host cells and cause disease and may contribute to different adherence mechanisms.

**GBS lysine lipids are important for the development of meningitis *in vivo***

Our results suggest that lysine lipids contribute to GBS invasion into brain endothelial cells. We hypothesized that this *in vitro* phenotype would translate into a diminished ability to penetrate the BBB and produce meningitis *in vivo*. Using our standard model of GBS hematogenous meningitis, mice were challenged with either WT GBS or the Δ*mprF* mutant as described in the Methods (13,37–40). Mice were sacrificed at a defined endpoint (72 h) to determine bacterial loads in blood and brain tissue. We recovered significantly less CFU in the brains of COH1Δ*mprF*-infected mice compared to the COH1-infected mice (Figure 8A). However, there was no significant difference in CFU recovered from the bloodstream between WT and mutant infected mice (Figure 8B). To assess the level of inflammation, we performed histological analysis of brains from infected animals. In WT-infected mice, we observed leukocyte infiltration and meningeal thickening characteristic of meningitis, which was less pronounced in the mice infected with the Δ*mprF* mutant strain (Figure 8C). Meningeal thickening was quantified as described in the methods (Figure 8D). Furthermore, consistent with these results, we observed that mice challenged with WT GBS had significantly more neutrophil chemokine, KC, in brain homogenates compared to Δ*mprF* mutant-infected animals (Figure 8E). Taken together,

these data indicate that *mprF* contributes to GBS penetration into the brain and to the pathogenesis of meningitis *in vivo*.

## Discussion

The cellular membrane is a critical site of interaction between Gram-positive pathogens and their hosts. In this study, we used LC-ESI/MS to characterize the lipid membranes of multiple serotypes of GBS. We identified Lys-Glc-DAG, a novel lysine modification on the glycolipid Glc-DAG, which comprises a relatively large proportion of the cellular lipid extract of these strains. We show that MprF is responsible for the addition of lysine to both Glc-DAG and PG, thus establishing a novel lipid substrate for MprF. We identified that these lysine lipids play important physiological roles in the GBS cellular membrane by masking negative charges, contributing to survival at a low pH, and impacting chain length. We further demonstrate that lysine lipid modification promotes GBS invasion into brain endothelium and contributes to the development of CNS disease in our mouse model of experimental meningitis. To our knowledge, this is the first description of the lysynylated glycolipid, Lys-Glc-DAG, in a bacterial pathogen that is important for host cell interactions and disease progression as well as a glucosyl-DAG substrate for an MprF enzyme.

Synthesis of Lys-PG and Lys-Glc-DAG by MprF reflects a complex balance of interconnected substrate usage including amino acid, glycolipid, and phospholipid substrates. Lys-tRNAs are required by translational machinery for protein synthesis and are essential for survival; unlike *S. aureus*, a canonical organism for studying MprF

function, GBS are lysine auxotrophs (33). Therefore, in GBS, both MprF and the ribosome would compete for lysine scavenged from the environment. Moreover, the Glc-DAG lipid, which is a substrate for GBS MprF, is also required for biosynthesis of the LTA anchor $Glc_2$-DAG; LTA is a critical polymer for binding host cells, repulsion of CAMPs, and is required for invasion of the BBB (2,13,41). Finally, GBS MprF acts on two substrates, PG and Glc-DAG, to synthesize two distinct lysine-modified lipids, the levels of all of which must be balanced to maintain appropriate membrane charge. In *E. faecium*, the hydrolase encoded immediately upstream of *mprF* is responsible for the turnover of Lys-PG in the membrane, thus balancing the amount of Lys-PG present (35). A similar mechanism is likely present in GBS to maintain the balance between both Lys-PG and Lys-Glc-DAG and their respective non-lysine decorated lipids. GBSCOH1_1932, immediately upstream of the GBS *mprF*, encodes the hydrolase domain MhpC (COG0596), indicating that it may regulate Lys-PG levels in the membrane; its activity on Lys-Glc-DAG is unknown. Overall, much remains to be determined about structural and biochemical properties of MprF and its regulation in GBS.

Currently, we are unable to decouple the functional roles of the two lysine-modified lipids as we show they are both synthesized by the GBS MprF. We have previously analyzed *E. faecium* lipids using the same methods here, and we experimentally confirmed that *E. faecium* synthesizes Lys-PG but not Lys-Glc-DAG (42). Swapping domains and regions between *E. faecium* MprF1 and GBS MprF may help to localize the region of GBS MprF responsible for binding the Glc-DAG substrate and/or generate variants of GBS MprF that synthesize only one of the two lysine-modified lipids. Decoupling the synthesis of Lys-PG

and Lys-Glc-DAG will allow further identification of the specific roles each lipid plays in GBS membrane function and pathogenesis. It is interesting to note that depending on lysine availability, GBS produce far more Lys-Glc-DAG than Lys-PG, as judged by LC/MS analysis. It is possible that that Lys-Glc-DAG can be more effectively used to modulate the charge-related biophysical and physiological properties of GBS membrane than Lys-PG.

Why did GBS evolve to use MprF to lysinylate Glc-DAG? The use of such an important substrate (lysine), required by GBS for protein synthesis, to decorate the extracellular cell surface is intriguing, especially under low lysine conditions *in vivo*. One possible explanation is to mask the recognition of Glc-DAG, an experimentally verified microbial antigen, from natural killer T cells (43,44). A second possible explanation is to increase resistance to neutrophil killing, as Lys-PG confers resistance to CAMPs in *S. aureus* (15); a role for GBS MprF in CAMP resistance was not observed in a previous study *in vitro* (14) but it may contribute under *in vivo* conditions. Finally, acid stress response that is greater with both lipids verses Lys-PG alone, may increase the survival time in phagosomes where acidification is critical for bacterial killing (45). Moreover, human vaginal tract colonization requires survival in low pH, as healthy adults have a pH range of 4.2 – 5 and the protective commensal *Lactobacillus* is known to acidify the surrounding environment (46,47). We show *in vitro* that the GBS lysine lipids play a critical role in survival at pH 5 and are also important for interactions with human vaginal epithelial cells. These data suggest that MprF and the lysine-modified lipids it synthesizes are especially important in the niches GBS colonizes, which requires further investigation. Additionally,

the decreased *in vivo* pathogenicity of the Δ*mprF* mutant presented in this work, identifies the GBS MprF as a strong candidate for targeting by anti-microbial strategies recently described in *S. aureus* (17,48). Finally, the fact that Lys-Glc-DAG is a unique and major membrane component of GBS holds promise that Lys-Glc-DAG could be utilized as a specific and efficient molecular biomarker for a rapid diagnostic test that would not rely on culturing procedures or nucleic acid amplification.

Overall, our work underscores the important roles of membrane lipids in pathogen-host interactions. Our identification of the novel Lys-Glc-DAG glycolipid and the joint role it plays with Lys-PG in GBS disease pathogenesis rationalizes further study of the lipidomes of human pathogens.

## Materials and methods

### Bacterial strains, media, and growth conditions

Strains and plasmids used in this study are shown in Supplementary Table 1. GBS strains were grown statically at 37°C in Todd-Hewitt Broth (THB) and *S. mitis* strains were grown statically at 37°C and 5% $CO_2$, unless otherwise stated. Streptococcal chemically defined medium (49) was diluted from stock as described (50) with 1% w/v glucose (referred to as DM), slightly modified from (51), unless otherwise stated. *Escherichia coli* strains were grown in Lysogeny Broth (LB) at 37°C with rotation at 225 rpm. Kanamycin and erythromycin (Sigma-Aldrich) were supplemented to media at 50 µg/mL and 300 µg/mL for *E. coli,* respectively, or 300 µg/mL and 5 µg/mL, respectively, for streptococcal strains.

**Routine molecular biology techniques**

All PCR reactions utilized Phusion polymerase (Thermo Fisher) and all primers are shown in Supplementary Table 2. PCR products and restriction digest products were purified using GeneJET PCR purification kit (Thermo Fisher) per manufacturer protocols. Plasmids were extracted using GeneJET plasmid miniprep kit (Thermo Fisher) per manufacturer protocols. Restriction enzyme digests utilized XbaI, XhoI, and PstI (New England Biolabs) for 3 h at 37°C in a water bath. Ligations utilized T4 DNA ligase (New England Biolabs) at 16°C overnight or Gibson Assembly Master Mix (New England Biolabs) per manufacturer protocols where stated. All plasmid constructs were sequence confirmed by Sanger sequencing (Massachusetts General Hospital DNA Core).

**Deuterated lysine and $^{13}C_6$-D-glucose isotope tracking**

A GBS COH1 colony was inoculated into 15 mL of DM containing 450 μM lysine-*d4* (Cambridge Isotopes Laboratories) or a single COH1 colony was inoculated into 10 mL DM supplemented with 0.5% w/v $^{13}C_6$D-glucose (U-13C6, Cambridge Isotopes Laboratories) for overnight growth for lipidomic analysis described below.

**Construction of MprF expression plasmids**

Genomic DNA was isolated using the Qiagen DNeasy Blood and Tissue kit per the manufacturer's protocol with the exception that cells were pre-treated with 180 μL 50 mg/mL lysozyme, 25 μL 2500 U/mL mutanolysin, and 15 μL 20 mg/mL pre-boiled RNase A and incubated at 37°C for 2 h. The *mprF* genes from GBS COH1, (GBSCOH1_1931), and *E. faecium* 1,231,410 (EFTG_00601 and EFTG_02430) were amplified and Gibson

ligated into pABG5Δ*phoZ* (31). Plasmid constructs were transformed into chemical competent *E. coli* DH5α cells. Briefly, chemically competent cells were incubated for 10 min on ice with 5 µL of Gibson reaction before heat shock at 42°C for 70 sec, then placed on ice for 2 min before 900 µL of cold SOC medium was added. Outgrowth was performed at 37°C, with shaking at 225 rpm, for 1 h. Cultures were plated on LB agar plates containing 50 µg/mL kanamycin. Colonies were screened by PCR for presence of the *mprF* insert.

**Expression of *mprF* in *S. mitis***

Natural transformation was performed as previously described (27). Briefly, precultures were thawed at room temperature, diluted in 900 µL of THB, further diluted 1:50 in prewarmed 5 mL THB, and incubated for 45 min at 37°C. 500 µL of culture was then aliquoted with 1 µL of 1 mg/ml competence-stimulating peptide (EIRQTHNIFFNFFKRR) and 1 µg/mL plasmid. Transformation reaction mixtures were cultured for 2 h at 37°C in microcentrifuge tubes before being plated on THB agar supplemented with 300 µg/mL kanamycin. Single transformant colonies were cultured in 15 mL THB overnight. PCR was used to confirm the presence of the *mprF* insert on the plasmid. Plasmids were extracted and sequence confirmed as described above. Lipidomics was performed as described below in biological triplicate.

**Construction of *mprF* deletion plasmid**

Regions ~2 kb upstream and downstream of the GBS COH1 *mprF* (GBSCOH1_1931) were amplified using PCR (Supplementary Table 2). Plasmid, pMBSacB (32), and the

PCR products were digested using appropriate restriction enzymes and ligated overnight. 7 µL of the ligation reaction was transformed into chemically competent *E. coli* DH5α as described above, except that outgrowth was performed at 28°C with shaking at 225 rpm for 90 min prior to plating on LB agar supplemented with 300 µg/mL erythromycin. Plates were incubated at 28°C for 72 h. Colonies were screened by PCR for correct plasmid construction. Positive colonies were inoculated into 50 mL LB media containing antibiotic and incubated at 28°C with rotation at 225 rpm for 72 h. Cultures were pelleted using a Sorvall RC6+ centrifuge at 4,280 x *g* for 6 min at room temperature. Plasmid was extracted as described above except the cell pellet was split into 5 columns to prevent overloading and serial eluted into 50 µL. Plasmid construction was confirmed via restriction digest using XhoI and XbaI, and the insert was PCR amplified and sequence-verified.

**Generation of electrocompetent *S. agalactiae* COH1 cells for knockout**

Electrocompetent cells were generated as described (32) with minor modifications. Briefly, a GBS COH1 colony was inoculated in 5 mL M17 medium (BD Bacto) with 0.5% glucose and grown overnight at 37°C. The 5 mL was used to inoculate a second overnight culture of 50 mL pre-warmed filter-sterilized M17 medium containing 0.5% glucose, 0.6% glycine, and 25% PEG 8000. The second overnight was added to 130 mL of the same medium and grown for 1 h at 37°C. Cells were pelleted at 3,200 x *g* in a Sorvall RC6+ at 4°C for 10 min. Cells were washed twice with 25 mL cold filter-sterilized GBS wash buffer containing 25% PEG 8000 and 10% glycerol in water, and pelleted as above. Cell pellets

were re-suspended in 1 mL GBS wash buffer and either used immediately for transformation or stored in 100 µL aliquots at -80°C until use.

**Deletion of GBS COH1 *mprF***

The double crossover homologous recombination knockout strategy was performed as described previously (32,37,52) with minor modifications. 1 µg of plasmid was added to electrocompetent COH1 cells and transferred to a cold 1 mm cuvette (Fisher). Electroporation was carried out at 2.5 kV on an Eppendorf eporator. 1 mL of THB containing 12.5% PEG 8000, 20 mM $MgCl_2$, and 2 mM $CaCl_2$ was immediately added and then the entire reaction was transferred to a glass culture tube. Outgrowth was at 28°C for 2 h followed by plating on THB agar supplemented with 5 µg/mL erythromycin. Plates were incubated for 48 h at 28°C. A single colony was cultured overnight in 5 mL THB with 5 µg/mL erythromycin at 28°C. The culture was screened via PCR for the plasmid insert with the initial denaturing step extended to 10 min. The overnight culture was diluted 1:1000 THB containing 5 µg/mL erythromycin and incubated overnight at 37°C to promote single cross over events. The culture was then serial diluted and plated on THB agar plates with antibiotic and incubated at 37°C overnight. Colonies were screened for single crossover events by PCR (Supplementary Table 2). Single crossover colonies were inoculated in 5 mL THB at 28°C to promote double crossover events. Overnight cultures were diluted 1:1000 into 5 mL THB containing sterile 0.75 M sucrose and incubated at 37°C. Overnight cultures were serial diluted and plated on THB agar and incubated at 37°C overnight. Colonies were patched onto THB agar with and without 5 µg/mL erythromycin to confirm loss of plasmid. Colonies were also screened by PCR

for the loss of *mprF*. Colonies positive for the loss of *mprF* were inoculated into 5 mL THB at 37°C. Cultures were stocked and gDNA extracted as described above, with minor modifications. Sequence confirmation of the *mprF* knockout was done via Sanger sequencing (Massachusetts General Hospital DNA Core) using primers in Supplementary Table 2. The mutant was grown overnight in 15 mL THB at 37°C and pelleted at 6,150 x *g* for 5 min in a Sorvall RC6+ centrifuge at room temperature for lipid extraction as described below. Genomic DNA of COH1Δ*mprF* was isolated as described above and whole genome sequencing was performed in paired-end reads (2 by 150 bp) on the Illumina NextSeq 550 platform at the Microbial Genome Sequencing Center (Pittsburgh, PA).

**Complementation of *mprF* in COH1Δ*mprF***

Electrocompetent COH1Δ*mprF* were generated as previously described (53). Briefly, COH1Δ*mprF* was inoculated into 5 mL THB with 0.6% glycine and grown overnight. The culture was expanded to 50 mL in pre-warmed THB with 0.6% glycine and grown to an $OD_{600}$ nm of 0.3 and pelleted for 10 min at 3200 x *g* at 4°C in a Sorvall RC6+ floor centrifuge. The pellet was kept on ice through the remainder of the protocol. The pellet was washed twice with 25 mL and once with 10 mL of cold 0.625 M sucrose and pelleted as above. The cell pellet was resuspended in 400 µL of cold 20% glycerol, aliquoted in 50 µL aliquots, and used immediately or stored at -80°C until use. Electroporation was performed as described above, with recovery in THB supplemented with 0.25 M sucrose, and plated on THB agar with kanamycin at 300 µg/mL.

**Acidic Bligh-Dyer extractions**

Centrifugation was performed using a Sorvall RC6+ centrifuge. Cultures were pelleted at 4,280 x *g* for 5 min at room temperature unless otherwise stated. The supernatants were removed, and cell pellets were stored at -80°C until acidic Bligh-Dyer lipid extractions were performed as described (27). Briefly, cell pellets were resuspended in 1X PBS (Sigma-Aldrich) and transferred to Coring Pyrex glass tubes with PTFR-lined caps (VWR), followed by 1:2 vol:vol chloroform:methanol addition. Single phase extractions were vortexed periodically and incubated at room temperature for 15 minutes before 500 x *g* centrifugation for 10 min. A two-phase Bligh-Dyer was achieved by addition of 100 µL 37% HCl, 1 mL $CHCl_3$, and 900 µl of 1X PBS, which was then vortexed and centrifuged for 5 min at 500 x *g.* The lower phase was removed to a new tube and dried under nitrogen before being stored at -80°C prior to lipidomic analysis.

**Liquid Chromatography/Electrospray Ionization Mass Spectrometry**

Normal phase LC was performed on an Agilent 1200 quaternary LC system equipped with an Ascentis silica HPLC column (5 µm; 25 cm by 2.1 mm; Sigma-Aldrich) as described previously (26,54). Briefly, mobile phase A consisted of chloroform-methanol-aqueous ammonium hydroxide (800:195:5, vol/vol), mobile phase B consisted of chloroform-methanol-water-aqueous ammonium hydroxide (600:340:50:5, vol/vol), and mobile phase C consisted of chloroform-methanol-water-aqueous ammonium hydroxide (450:450:95:5, vol/vol). The elution program consisted of the following: 100% mobile phase A was held isocratically for 2 min, then linearly increased to 100% mobile phase B over 14 min, and held at 100% mobile phase B for 11 min. The LC gradient was then

changed to 100% mobile phase C over 3 min, held at 100% mobile phase C for 3 min, and, finally, returned to 100% mobile phase A over 0.5 min and held at 100% mobile phase A for 5 min. The LC eluent (with a total flow rate of 300 µl/min) was introduced into the ESI source of a high-resolution TripleTOF5600 mass spectrometer (Sciex, Framingham, MA). Instrumental settings for negative-ion ESI and MS/MS analysis of lipid species were: IS = -4,500 V, CUR = 20 psi, GSI = 20 psi, DP = -55 V, and FP = -150V. Settings for positive-ion ESI and MS/MS analysis were: IS = +5,000 V, CUR = 20 psi, GSI = 20 psi, DP = +55 V, and FP = +50V. The MS/MS analysis used nitrogen as the collision gas. Data analysis was performed using Analyst TF1.5 software (Sciex, Framingham, MA).

**Growth curves**

Overnight cultures were used to inoculate a 96 well flat-bottom plate (Falcon) at an $OD_{600nm}$ of ~0.02 in a final volume of 200 µL THB. Plates were grown in a Biotek MX Synergy 2.0 plate reader at 37°C with $OD_{600nm}$ readings every 15 minutes for 15 h. Growth curves were performed in biological triplicate.

**Cytochrome C assay**

Cytochrome C assay was performed as described previously (55,56) with minor modifications. Briefly, overnight cultures of strains were diluted to an $OD_{600nm}$ of 0.05 in 20 mL prewarmed THB, with no antibiotic, and grown to mid exponential phase ($OD_{600nm}$ between 0.48 – 0.6) before cells were pelleted to an $OD_{600nm}$ of 7 in 1 mL and washed twice with morpholinepropanesulfonic acid (MOPS) at pH 7. Cells were resuspended in

1 mg/mL Cytochrome C (Sigma) in MOPS buffer and incubated for 10 min at room temperature. Cells were pelleted at 16,000 x *g* for 3 min in a tabletop centrifuge, supernatant transferred to disposable spectrophotometer cuvette (Fisher), and absorbance read at 535nm ($A_{535}$) using a Thermo Scientific Genesys 30 spectrophotometer. The control $A_{535}$ was 1 mg/mL Cytochrome C in MOPS buffer with no cells present, which was also incubated and centrifuged. % bound was calculated using the following formula: (100 – ($A_{535}$/Control $A_{535}$)) * 100. Biological triplicate was used for each strain.

**pH-adjusted THB growth**

Approximately 30 mL of fresh THB were adjusted to different pH values, measured using a Mettler Toledo FiveEasy pH/MV meter, and sterile-filtered using 0.22 µM syringe filters. A final volume of 200 µL culture medium was aliquoted per well in a flat-bottom 96 well plate (Falcon); culture media were not supplemented with antibiotics. Overnight cultures of GBS strains were used to inoculate the wells to a starting $OD_{600nm}$ 0.02 per well. Plates were incubated for 24 h at 37°C before $OD_{600nm}$ was read using a BioTek MX Synergy 2 plate reader. This experiment was performed in biological triplicate.

**Hemolytic assay**

Hemolytic assays were performed as described ((38)) with minor modifications. Briefly, strains were grown to an $OD_{600nm}$ of ~0.4, pelleted at 16,000 *x g* in an Eppendorf 5415D tabletop centrifuge, and resuspended in PBS. ~8-9 x $10^7$ CFU in 20 µL PBS was added to 230 µL fresh sheep blood (VWR) in U-bottom 96-well plates (Corning) for a final volume

of 250 μL per well. Control wells were treated with 20 μL sterile water. The plates were sealed and incubated at 37°C with rotation at 100 rpm for 1 h. The plates were centrifuged at 400 x g for 10 min in an Eppendorf 5810 tabletop centrifuge, and 100 μL of the supernatant was transferred to a flat-bottom 96-well plate (Falcon). 50 μL was diluted 1:2 in PBS and the absorbance at 541 nm ($A_{541}$) was read using a BioTek MX Synergy 2 plate reader. Percent hemolysis was calculated by comparing the $A_{541}$ of GBS treated wells to those of wells treated with water. Biological and technical replicates were performed for each strain.

**Membrane dye and imaging of GBS**

Overnight cultures were gently resuspended 5 times by pipette. 19 μL culture was removed into sterile Eppendorf tubes. 1 μL of 1 μg/mL FM4-64 (N-(3-Triethylammoniumpropyl)-4-(6-(4-(Diethylamino) Phenyl) Hexatrienyl) Pyridinium Dibromide) membrane dye (Invitrogen) was added to each tube. The culture and dye were dropped onto a 0.75 mm 0.75% agarose pad and allowed to stand for 5 min. Cover slips were placed and sealed. A Zeiss LSM 880 confocal microscope was used for imaging with 100X objective, oil immersion, and laser excitation at 561 nm. Settings of laser power 1%, gain 750, digital offset 0 and digital gain 1 were used for each image. Five representative images were taken from each slide and the number of diplococci occurring in each chain was manually counted.

**hCMEC and VK2 cell adherence and invasion assays**

Human Cerebral Microvascular Endothelial cells hCMEC/D3 (obtained from Millipore) were grown in EndoGRO-MV complete media (Millipore, SCME004) supplemented with 5% fetal bovine serum (FBS) and 1 ng/ml fibroblast growth factor-2 (FGF-2; Millipore). Human vaginal epithelial VK2/E6E7 (obtained from American Type Culture Collection (ATCC) (CRL-2616)) cells were grown in keratinocyte serum-free medium (KSFM) (Gibco) supplemented with 0.5 ng/mL human recombinant epidermal growth factor and 0.05 mg/mL bovine pituitary extract. Cells were grown in tissue culture treated 24 well plates and 5% $CO_2$ at 37°C.

Assays to determine the total number of bacteria adhered to host cells or intracellular bacteria were performed as described previously (37,38). Briefly, bacteria were grown to mid log phase ($OD_{600nm}$ 0.4-0.5) and normalized to 1 x $10^8$ to infect cell monolayers at a multiplicity of infection (MOI) of 1 (1 x $10^5$ CFU per well). The total cell-associated GBS were recovered after 30 min incubation. Cells were washed slowly five times with 500 µL 1X PBS (Sigma) and detached by addition of 100 µL of 0.25% trypsin-EDTA solution (Gibco) and incubation for 5 min before lysing the eukaryotic cells with the addition of 400 µL of 0.025% Triton X-100 (Sigma) and vigorous pipetting. The lysates were then serially diluted and plated on THB agar and incubated overnight to determine CFU. Bacterial invasion assays were performed as described above except infection plates were incubated for 2 h before incubation with 100 µg gentamicin (Sigma) and 5 µg penicillin (Sigma) supplemented media for an additional 2 h to kill all extracellular bacteria, prior to

being trypsinized, lysed, and plated as described. Experiments were performed in biological triplicate with four technical replicates per experiment.

**Murine model of GBS hematogenous meningitis**

All animal experiments were conducted under the approval of the Institutional Animal Care and Use Committee (#00316) at the University of Colorado Anschutz Medical Campus and performed using accepted veterinary standards. The murine meningitis model was performed as previously described (37,39,40). Briefly, 7-week-old male CD1 (Charles River) mice were challenged intravenously with $1 \times 10^9$ CFU of WT COH1 or the isogenic Δ*mprF* mutant. At 72 h post-infection, mice were euthanized and blood and brain tissue were harvested, homogenized, and serially diluted on THB agar plates to determine bacterial CFU.

**Histology and ELISA**

Mouse brain tissue was frozen in OCT compound (Sakura) and sectioned using a CM1950 cryostat (Leica). Sections were stained using hematoxylin and eosin (Sigma) and images were taken using a BZ-X710 microscope (Keyence). Images were analyzed using ImageJ software. Meningeal thickening was quantified from sections taken from three different mice per group, and six images per slide. Meningeal thickening was quantified across two points per image. KC protein from mouse brain homogenates was detected by enzyme-linked immunosorbent assay according to the manufacturer's instructions (R&D systems).

## Statistical analyses

All statistical analyses were performed using GraphPad Prism version 8 for Windows, GraphPad Software, La Jolla California USA, www.graphpad.com.

## Mouse study approval

All animal experiments were conducted under the approval of the Institutional Animal Care and Use Committee (protocol #00316) at the University of Colorado Anschutz Medical Campus and performed using accepted veterinary standards.

## Accession numbers

Illumina sequence reads generated in this study have been deposited in the Sequence Read Archive under accession PRJNA675025.

## Author contributions

LJ, ZG, and KP designed the experiments, except for human cell line and mouse infection work designed by HM and KD. LJ performed all experiments, besides human cell line work performed by HM, mouse infection work performed by HM, JM, and RV, and lipidomic analyses performed by ZG. This manuscript was written by LJ, with exception of the mass spectrometry identification section by ZG, and edited by LJ, ZG, KD and KP.

**Acknowledgements**

We gratefully acknowledge Kathryn Patras at the University of California San Diego for the CNCTC 10/84 strain and Moutusee Islam in Kelli Palmer's lab at The University of Texas at Dallas for the *E. faecium* 1,231,410 genomic DNA used for PCR amplification.

The work was supported in part by T32 5T32AI052066-18 for H.S.M, the Coordenação de Aperfeiçoamento de Pessoal de Nível Superior, Brazil (CAPES; finance code 001 to J.D.C.M), by grant R01NS116716 from the National Institutes of Health to K.S.D and associated supplement from NINDS to R.V., by grant R21AI130666 from the National Institutes of Health and the Cecil H. and Ida Green Chair in Systems Biology Science to K.P, grant R56AI139105 from the National Institutes of Health to K.P and Z.G, and grant U54GM069338 from the National Institutes of Health to Z.G.

**References**

1. Wilkinson HW. Group B Streptococcal Infection in Humans. *Annu Rev Microbiol*. 1978;32(1):41-57.
2. Doran KS, Nizet V. Molecular pathogenesis of neonatal Group B Streptococcal infection: No longer in its infancy. *Mol Microbiol*. 2004;54(1):23-31.
3. Hall J, et al. Maternal Disease With Group B *Streptococcus* and Serotype Distribution Worldwide: Systematic Review and Meta-analyses. *Clin Infect Dis*. 2017;65(suppl_2):S112-S124.
4. Schuchat A. Group B Streptococcus. *Lancet*. 1999;353:51-56.
5. Campbell JR, Hillier SL, Krohn MA, Ferrieri P, Zaleznik DF, Baker CJ. Group B

streptococcal colonization and serotype-specific immunity in pregnant women at delivery. *Obstet Gynecol*. 2000;96(4):498-503.

6. Nandyal RR. Update on group B streptococcal infections: perinatal and neonatal periods. *J Perinat Neonatal Nurs*. 2008;22(3):230-237.
7. Edwards MS, Rench MA, Haffar AA, Murphy MA, Desmond MM, Baker CJ. Long-term sequelae of group B streptococcal meningitis in infants. *J Pediatr*. 1985;106(5):717-722.
8. Schuchat A. Epidemiology of Group B Streptococcal disease in the United States: shifting paradigms. *Clin Microbiol Rev*. 1998;11(3):497-513.
9. Ohlsson A, Shah VS. Intrapartum antibiotics for known maternal Group B Streptococcal colonization. *Cochrane database Syst Rev*. 2014;(6):CD007467.
10. Armistead B, Oler E, Adams Waldorf K, Rajagopal L. The Double Life of Group B Streptococcus: Asymptomatic Colonizer and Potent Pathogen. *J Mol Biol*. 2019;431(16):2914-2931.
11. Curtis J, Kim G, Wehr NB, Levine RL. Group B Streptococcal phospholipid causes pulmonary hypertension. *Proc Natl Acad Sci U S A*. 2003;100(9):5087-5090.
12. Fischer W. The polar lipids of Group B Streptococci. II. Composition and positional distribution of fatty acids. *Biochim Biophys Acta*. 1977;487(1):89-104.
13. Doran KS, et al. Blood-brain barrier invasion by Group B Streptococcus depends upon proper cell-surface anchoring of lipoteichoic acid. *J Clin Invest*. 2005;115(9):2499-2507.
14. Saar-Dover R, et al. D-alanylation of lipoteichoic acids confers resistance to

cationic peptides in Group B *Streptococcus* by increasing the cell wall density. Peschel A, ed. *PLoS Pathog*. 2012;8(9):e1002891.

15. Peschel A, et al. *Staphylococcus aureus* resistance to human defensins and evasion of neutrophil killing via the novel virulence factor MprF is based on modification of membrane lipids with L-lysine. *J Exp Med*. 2001;193(9):1067-1076.
16. Roy H, Ibba M. RNA-dependent lipid remodeling by bacterial multiple peptide resistance factors. *Proc Natl Acad Sci U S A*. 2008;105(12):4667-4672.
17. Ernst CM, et al. The Lipid-Modifying Multiple Peptide Resistance Factor Is an Oligomer Consisting of Distinct Interacting Synthase and Flippase subunits. *MBio*. 2015;6(1):1-9.
18. Roy H, Ibba M. Broad range amino acid specificity of RNA-dependent lipid remodeling by multiple peptide resistance factors. *J Biol Chem*. 2009;284(43):29677-29683.
19. Hebecker S, et al. Structures of two bacterial resistance factors mediating tRNA-dependent aminoacylation of phosphatidylglycerol with lysine or alanine. *Proc Natl Acad Sci U S A*. 2015;112(34):10691-10696.
20. Slavetinsky C, Kuhn S, Peschel A. Bacterial aminoacyl phospholipids - Biosynthesis and role in basic cellular processes and pathogenicity. *Biochim Biophys acta Mol cell Biol lipids*. 2017;1862(11):1310-1318.
21. Kuypers JM, Heggen LM, Rubens CE. Molecular analysis of a region of the Group B Streptococcus chromosome involved in type III capsule expression. *Infect Immun*. 1989;57(10):3058-3065.

22. Lancefield RC, McCarty M, Everly WN. Multiple mouse-protective antibodies directed against group B streptococci. Special reference to antibodies effective against protein antigens. *J Exp Med*. 1975;142(1):165-179.

23. Wilkinson HW. Nontypable group B streptococci isolated from human sources. *J Clin Microbiol*. 1977;6(2):183-184.

24. Hooven TA, et al. Complete Genome Sequence of *Streptococcus agalactiae* CNCTC 10/84, a Hypervirulent Sequence Type 26 Strain. *Genome Announc*. 2014;2(6).

25. Bligh EG, Dyer WJ. A Rapid Method of Total Lipid Extraction and Purification. *Can J Biochem Physiol*. 1959;37(8):911-917.

26. Tan BK, Bogdanov M, Zhao J, Dowhan W, Raetz CRH, Guan Z. Discovery of a cardiolipin synthase utilizing phosphatidylethanolamine and phosphatidylglycerol as substrates. *Proc Natl Acad Sci*. 2012;109(41):16504-16509.

27. Joyce LR, Guan Z, Palmer KL. Phosphatidylcholine Biosynthesis in Mitis Group Streptococci via Host Metabolite Scavenging. *J Bacteriol*. 2019;201(22):e00495-19.

28. Yalcin T, Harrison AG. Ion chemistry of protonated lysine derivatives. *J Mass Spectrom*. 1996;31(11):1237-1243.

29. Meiers M, Volz C, Eisel J, Maurer P, Henrich B, Hakenbeck R. Altered lipid composition in Streptococcus pneumoniae cpoA mutants. *BMC Microbiol*. 2014;14(1):1-12.

30. Adams HM, Joyce LR, Guan Z, Akins RL, Palmer KL. Streptococcus mitis and S. oralis Lack a Requirement for CdsA, the Enzyme Required for Synthesis of Major

Membrane Phospholipids in Bacteria. *Antimicrob Agents Chemother*. 2017;61(5):e02552-16.

31. Granok AB, Parsonage D, Ross RP, Caparon MG. The RofA binding site in *Streptococcus pyogenes* is utilized in multiple transcriptional pathways. *J Bacteriol*. 2000;182(6):1529-1540.

32. Hooven TA, Bonakdar M, Chamby AB, Ratner AJ. A Counterselectable Sucrose Sensitivity Marker Permits Efficient and Flexible Mutagenesis in *Streptococcus agalactiae*. *Appl Environ Microbiol*. 2019;85(7):1-13.

33. Milligan TW, Doran TI, Straus DC, Mattingly SJ. Growth and amino acid requirements of various strains of Group B Streptococci. *J Clin Microbiol*. 1978;7(1):28-33.

34. Wishart DS, et al. HMDB 4.0: the human metabolome database for 2018. *Nucleic Acids Res*. 2018;46(D1):D608-D617.

35. Smith AM, Harrison JS, Sprague KM, Roy H. A conserved hydrolase responsible for the cleavage of aminoacylphosphatidylglycerol in the membrane of *Enterococcus faecium*. *J Biol Chem*. 2013;288(31):22768-22776.

36. Roy H. Tuning the properties of the bacterial membrane with aminoacylated phosphatidylglycerol. *IUBMB Life*. 2009;61(10):940-953.

37. Spencer BL, et al. Cas9 contributes to Group B Streptococcal colonization and disease. *Front Microbiol*. 2019;10(AUG):1-15.

38. Deng L, et al. The Group B Streptococcal surface antigen I/II protein, BspC, interacts with host vimentin to promote adherence to brain endothelium and inflammation during the pathogenesis of meningitis. *PLoS Pathog*. 2019;15(6):1-

30.

39. Banerjee A, et al. Bacterial Pili exploit integrin machinery to promote immune activation and efficient blood-brain barrier penetration. *Nat Commun*. 2011;2(1):462.

40. Kim BJ, et al. Bacterial induction of Snail1 contributes to blood-brain barrier disruption. *J Clin Invest*. 2015;125(6):2473-2483.

41. Poyart C, et al. Attenuated virulence of *Streptococcus agalactiae* deficient in D-alanyl-lipoteichoic acid is due to an increased susceptibility to defensins and phagocytic cells. *Mol Microbiol*. 2003;49(6):1615-1625.

42. Bhardwaj P, Hans A, Ruikar K, Guan Z, Palmer KL. Reduced Chlorhexidine and Daptomycin Susceptibility in Vancomycin-Resistant *Enterococcus faecium* after Serial Chlorhexidine Exposure. *Antimicrob Agents Chemother*. 2018;62(1).

43. Kinjo Y, et al. Invariant natural killer T cells recognize glycolipids from pathogenic Gram-positive bacteria. *Nat Immunol*. 2011;12(10):966-974.

44. Zajonc DM, Girardi E. Recognition of microbial glycolipids by Natural Killer T cells. *Front Immunol*. 2015;6(JUL):1-11.

45. Flannagan RS, Cosío G, Grinstein S. Antimicrobial mechanisms of phagocytes and bacterial evasion strategies. *Nat Rev Microbiol*. 2009;7(5):355-366.

46. Miller EA, Beasley DAE, Dunn RR, Archie EA. Lactobacilli dominance and vaginal pH: Why is the human vaginal microbiome unique? *Front Microbiol*. 2016;7(DEC).

47. Neugent ML, Hulyalkar N V., Nguyen VH, Zimmern PE, De Nisco NJ. Advances in Understanding the Human Urinary Microbiome and Its Potential Role in Urinary Tract Infection. *MBio*. 2020;11(2).

48. Slavetinsky CJ, et al. Decoding and blocking the bacterial lipid flippase MprF yields a novel anti-virulence strategy [preprint]. https://doi.org/10.1101/2020.11.12.379776. Posted on bioRxiv November 14, 2020.

49. Van De Rijn I, Kessler RE. Growth characteristics of Group A Streptococci in a new chemically defined medium. *Infect Immun*. 1980;27(2):444-448.

50. Chang JC, LaSarre B, Jimenez JC, Aggarwal C, Federle MJ. Two Group A Streptococcal peptide pheromones act through opposing rgg regulators to control biofilm development. *PLoS Pathog*. 2011;7(8):e1002190.

51. Gupta R, Shah P, Swiatlo E. Differential gene expression in *Streptococcus pneumoniae* in response to various iron sources. *Microb Pathog*. 2009;47:101-109.

52. Holo H, Nes IF. High-frequency transformation, by electroporation, of *Lactococcus lactis* subsp. *cremoris* grown with glycine in osmotically stabilized media. *Appl Environ Microbiol*. 1989;55(12):3119-3123.

53. Framson PE, Nittayajarn A, Merry J, Youngman P, Rubens CE. New genetic techniques for Group B Streptococci: High-efficiency transformation, maintenance of temperature-sensitive pWV01 plasmids, and mutagenesis with Tn917. *Appl Environ Microbiol*. 1997;63(9):3539-3547.

54. Li C, Tan BK, Zhao J, Guan Z. In vivo and in vitro synthesis of phosphatidylglycerol by an Escherichia coli cardiolipin synthase. *J Biol Chem*. 2016;291(48):25144-25153.

55. Gogos A, Jimenez J, Chang J, Wilkening R, Federle M. A Quorum Sensing-

Regulated Protein Binds Cell Wall *Streptococcus pyogenes*. *J Bacteriol*. 2018;200(11):1-16.

56. Kristian SA, et al. D-alanylation of teichoic acids promotes Group A *Streptococcus* antimicrobial peptide resistance, neutrophil survival, and epithelial cell invasion. *J Bacteriol*. 2005;187(19):6719-6725.

57. Garrett TA, Raetz CRH, Son JD, Richardson TD, Bartling C, Guan Z. Non-enzymatically derived minor lipids found in Escherichia coli lipid extracts. *Biochim Biophys Acta*. 2011;1811(11):827-837.

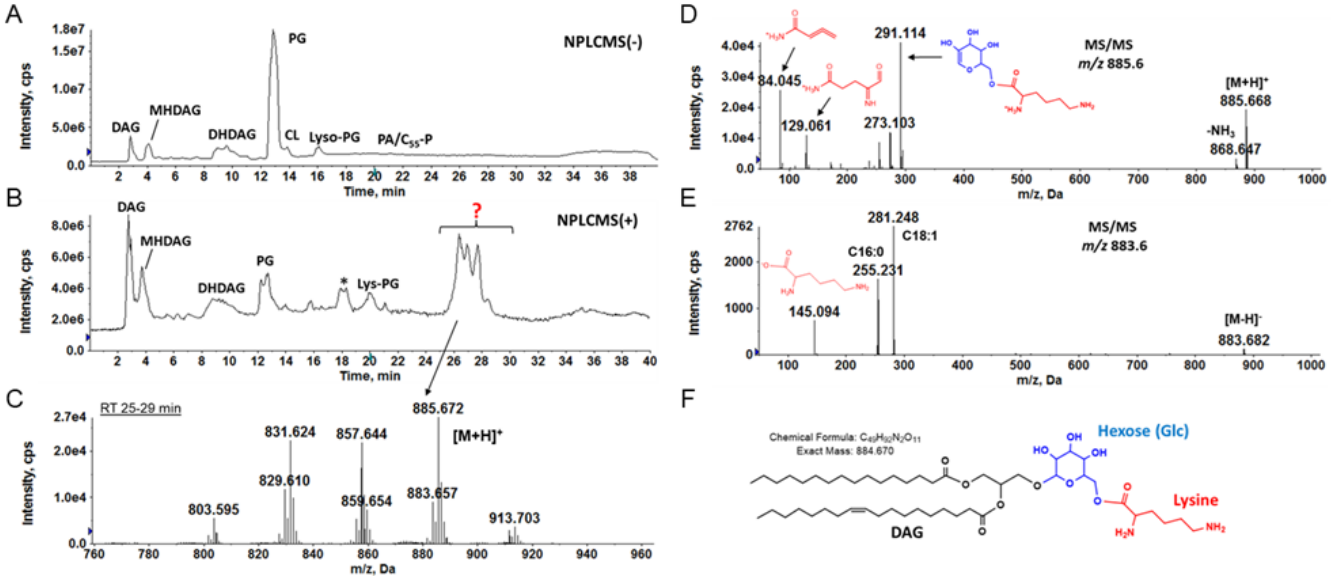


**Figure 1. Lipidomic profiling identifies a major unknown lipid as Lysyl-Glucosyl-Diacylglycerol in GBS.** The total lipid extract of the WT COH1 strain was analyzed by normal phase LC-ESI/MS in both negative and positive ion modes. A) Total ion chromatogram (TIC) of LC/MS in the negative ion mode shows common Gram-positive bacterial lipids. B) TIC of LC/MS in the positive ion mode shows a major unknown lipid eluting from the column at ~25 to 29 min. C) Positive ESI/MS showing the $[M+H]^+$ ions of the unknown lipid. The spectrum was averaged from those acquired during the retention time of 25 to 29 min. D) Positive ion MS/MS spectrum of $[M+H]^+$ at *m/z* 885.6 of the unknown lipid. E) Negative ion MS/MS spectrum of $[M-H]^-$ at *m/z* 883.6 of the unknown lipid. F) Lys-Glc-DAG (16:0/18:1) is proposed as the structure of the unknown lipid that gave rise to the $[M+H]^+$ at *m/z* 885.6 and $[M-H]^-$ at *m/z* 883.6. The hexose was assigned as glucose, because glucosyl-DAG is a major gram-positive membrane lipid and is supported by the isotopic labeling studies using a $^{13}C$-labeled glucose shown below. The acyl chain compositions and exact masses of Lys-Glc-DAG molecular species observed in COH1 are listed in Table 2. "*" denotes methylcarbamate of Lys-Glc-DAG , an extraction artifact due to the use of chloroform (57).

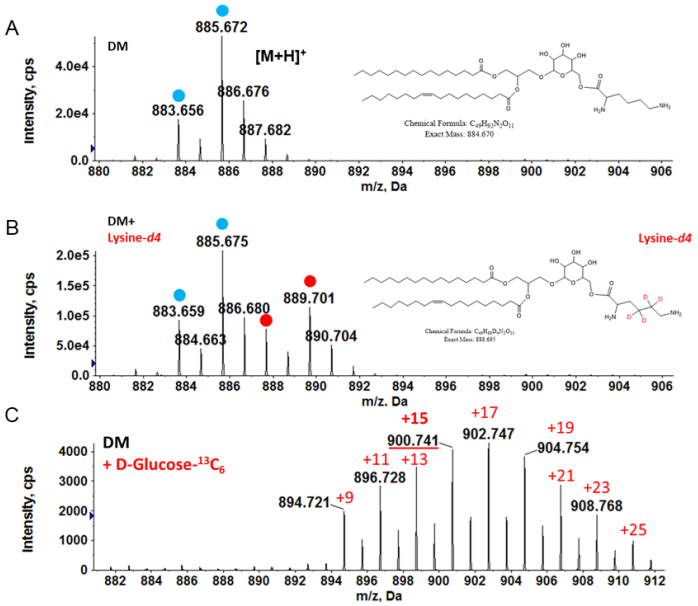


**Figure 2. Isotopic incorporation of deuterated lysine and $^{13}$C-labeled glucose into Lys-Glc-DAG.** The lipid extracts of COH1 cultured in DM, DM supplemented with 450 μM L-lysine-*d4* (4,4,5,5-D4), or in DM containing 0.5% w/v D-Glucose (U-$^{13}C_6$) were analyzed by LC-ESI/MS in the positive ion mode. A) $[M+H]^+$ ions of major Lys-Glc-DAG species in COH1 cultured in DM. B) $[M+H]^+$ ions of major Lys-Glc-DAG species in COH1 cultured in DM supplemented with lysine-*d4.* The incorporation of lysine-*d4* in Lys-Glc-DAG is evidenced by an upward *m/z* shift of 4 Da from unlabeled Lys-Glc-DAG (blue dots) to labeled Lys-Glc-DAG (red dots). C) $[M+H]^+$ ion of Lys-Glc-DAG (16:0/18:1) is observed at multiple peaks with higher m/z values (from *m/z* 894.7 to 910.8) when *S. agalactiae* COH1 is cultured in DM supplemented with D-Glucose-$^{13}C_6$. The mass shifts, ranging from +9 to +25 Da, indicate the numbers of $^{13}$C atoms that were incorporated into Lys-Glc-DAG (16:0/18:1).

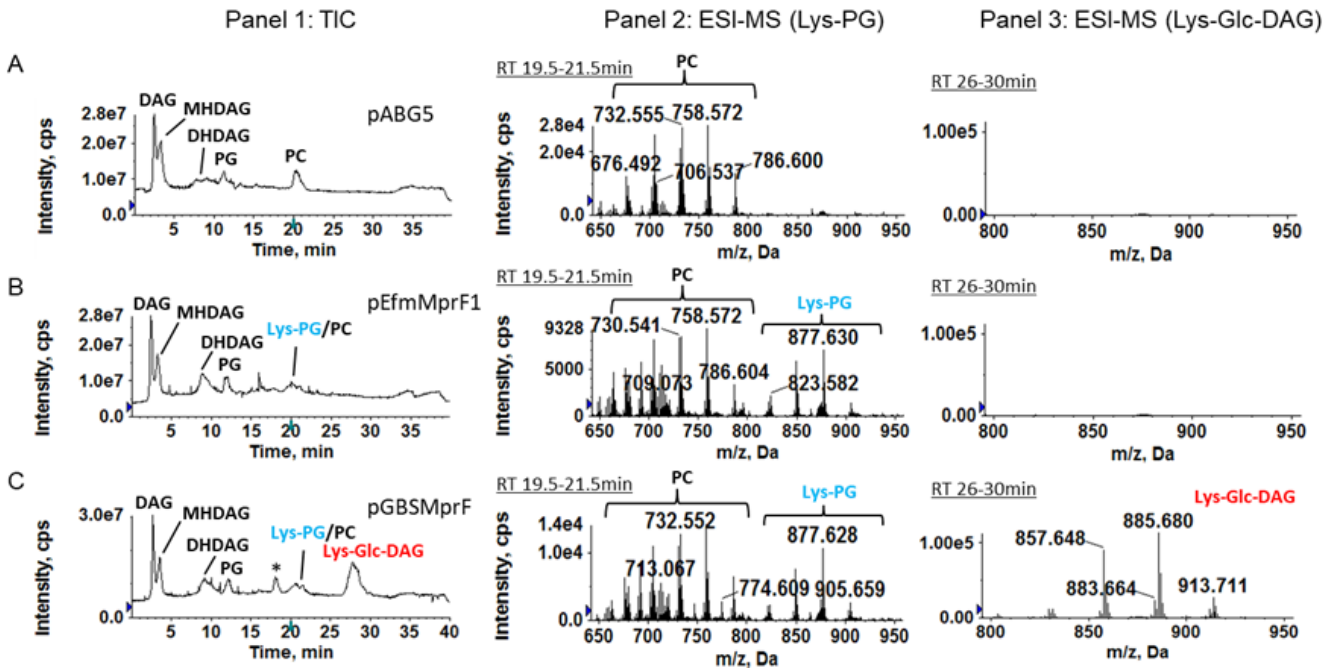


**Figure 3. Expression of *E. faecium* MprF and GBS MprF in *S. mitis*.** The lipid extracts of *S. mitis* ATCC 49456 cells with empty vector control (pABG5), expressing *E. faecium mprF1* (pEfmMprF1), and GBS *mprF* (pGBSMprF), were analyzed by LC-ESI/MS in the positive ion mode. Panel 1: Total ion chromatograms (TIC), Panel 2: Mass spectra (MS) of retention time 19.5 – 21.5 min showing Lys-PG, and Panel 3: MS of retention time 26 – 30 min for Lys-Glc-DAG. A) *S. mitis* (pABG5), B) *S. mitis* (pEfmMprF1), and C) *S. mitis* (pGBSMprF). Phosphatidylcholine (PC) elutes around the same retention time of Lys-PG. Lys-PG is present when *mprF* from either *E. faecium* or GBS are expressed. Lys-Glc-DAG is only synthesized by the GBS MprF, indicating two lipid substrates for the GBS MprF. "*" denotes methylcarbamate of Lys-Glc-DAG, an extraction artifact.

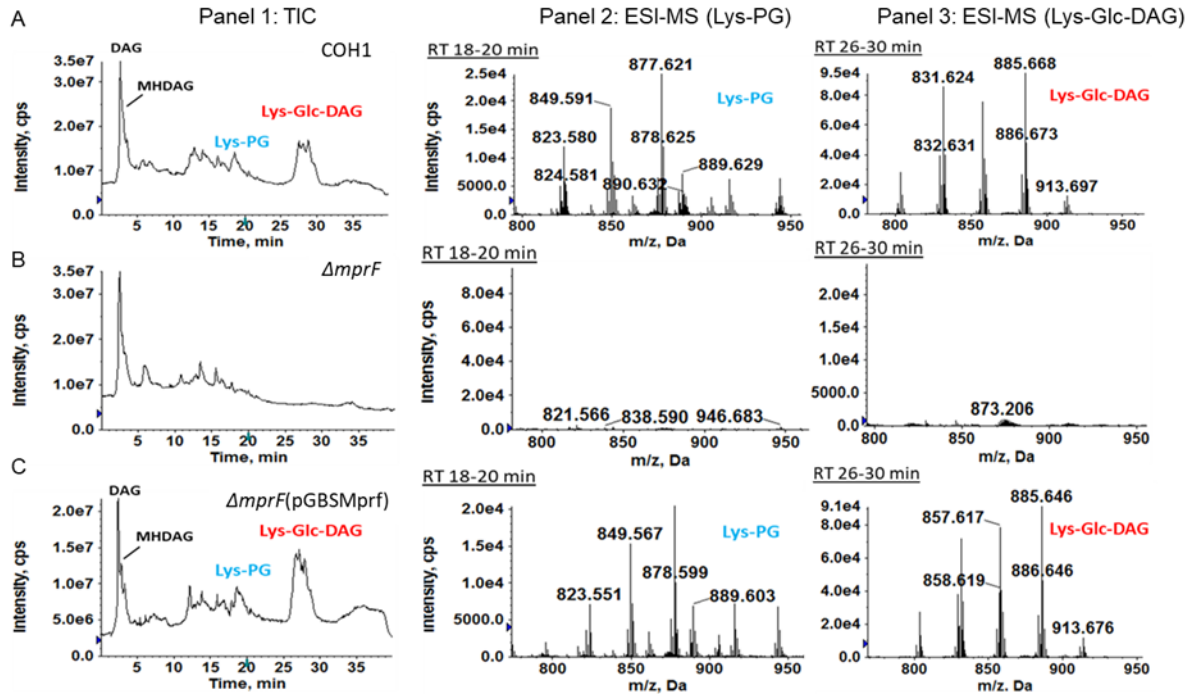


**Figure 4. Deletion of *mprF* (GBSCOH1_1931) results in the loss of both Lys-PG and Lys-Glc-DAG from GBS.** The lipid extracts of COH1 WT, COH1Δ*mprF* and Δ*mprF* (pGBSMprF) complement were analyzed by LC-ESI/MS in the positive ion mode. Panel 1: Total ion chromatograms (TIC), Panel 2: Mass spectra of retention time 18 – 20 min showing Lys-PG, and Panel 3: Mass spectra of retention time 26 – 30 min for Lys-Glc-DAG. A) COH1 WT, B) COH1Δ*mprF*, and C) Δ*mprF* (pGBSMprF) complement. The deletion of *mprF* from the COH1 genome results in a complete loss of both Lys-PG and Lys-Glc-DAG from the membrane, with both being restored in the complement strain, confirming MprF is the biosynthetic enzyme of both Lys-PG and Lys-Glc-DAG.

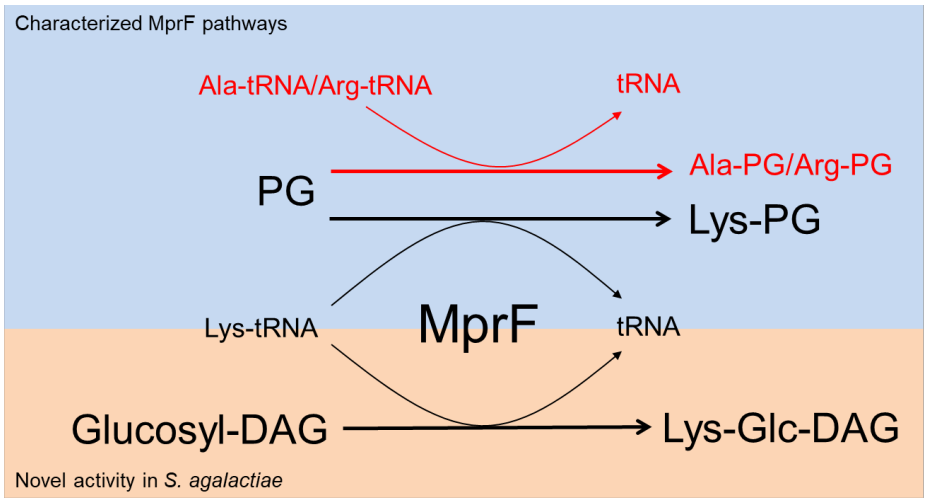


**Figure 5. Biosynthetic pathways involving MprF**. MprF has been demonstrated to catalyze the formation of Ala-PG, Arg-PG, and Lys-PG in many bacterial species (blue shading). In this study, we discover a novel function of MprF in GBS in the formation of Lys-Glc-DAG (orange shading). The biosynthetic pathways of MprF in GBS are denoted in black. Ala-PG and Arg-PG (formed by the pathway denoted in red) are not detected in GBS.

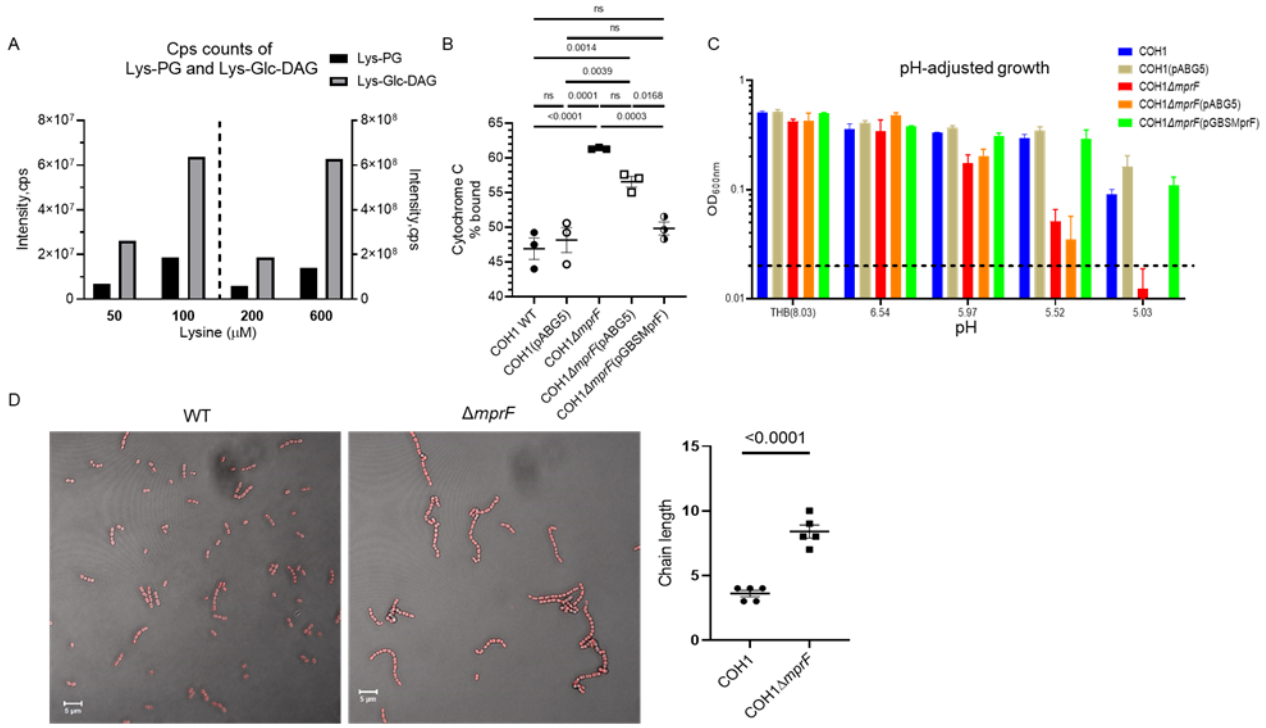


**Figure 6. Lysine titration and COH1Δ*mprF* surface charge, acid tolerance, and chain length.** A) Counts per second (CPS) counts from mass spectra for Lys-PG and Lys-Glc-DAG molecular species at each concentration. B) Mean percent Cytochrome C bound to COH1 WT, WT containing the empty vector pABG5, Δ*mprF* mutant, Δ*mprF* mutant containing the empty vector, and the pGBSMprF complement strains. The Δ*mprF* mutant displays significantly more Cytochrome C bound to the cells, indicating a more net negative outer surface charge. C) Growth yields ($OD_{600nm}$) after overnight culture in pH-adjusted THB broth. The Δ*mprF* mutant is more susceptible to the lower pH and fails to grow at pH 5 compared to the WT and complement. Dashed line represents starting inoculum of $OD_{600nm}$ ~0.02. D) Representative image of stationary phase COH1 WT and Δ*mprF* mutant stained with membrane dye FM4-64 and manual counts of the number of diplococci in each chain imaged in the 5 images taken from each slide. Scale bar is 5 μm. B) and D) Mean and SEM, C) Mean and SD indicated. Statistical analysis: B) One-way ANOVA with Tukey's multiple comparisons test, D) unpaired two-tailed t-test, p-values indicated.

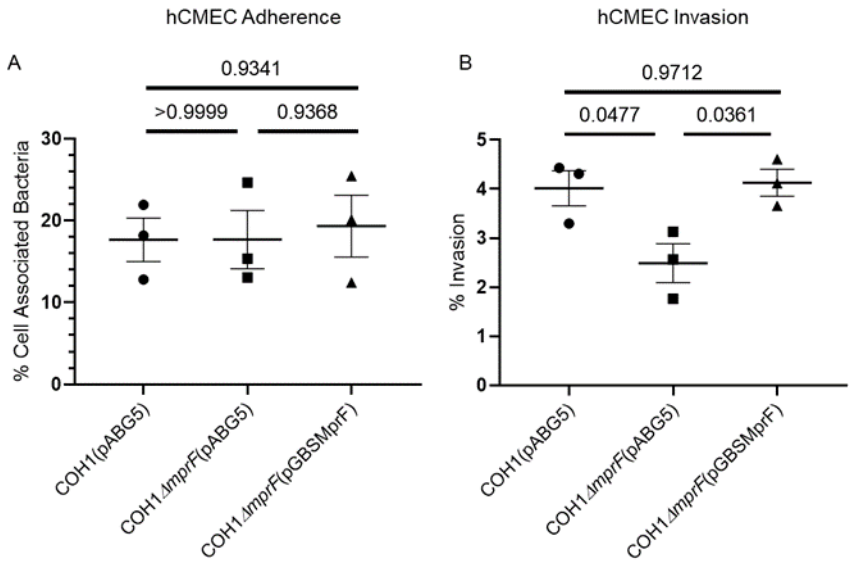


**Figure 7. MprF contributes to GBS invasion, but not adhesion, of human endovascular cell line *in vitro***. COH1(pABG5), Δ*mprF*(pABG5), and complement strain Δ*mprF*(pGBSMprF) were tested for A) adhesion and B) invasion of the human cerebral endovascular hCMEC/DE3 cell line. The Δ*mprF*(pABG5) strain displays no significant difference in adhesion but a significant difference in invasion of the endovascular cell line when compared to WT and complement strains. *In vitro* tissue culture assay results are the mean of three replicate experiments, each with four technical replicates. Mean and SEM indicated, statistical analyses: One-way ANOVA with Tukey's multiple comparisons test, p-values indicated.

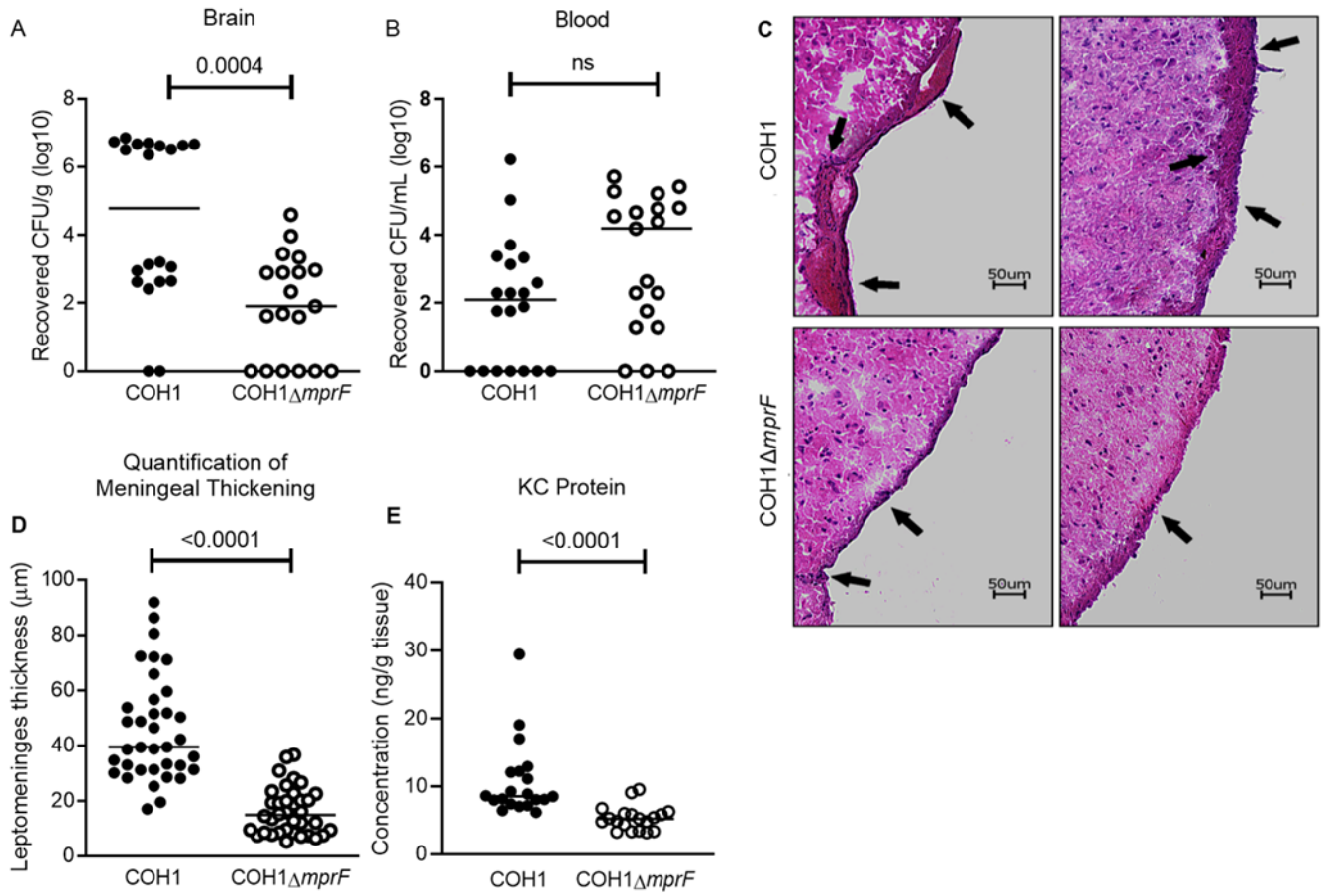


**Figure 8. MprF contributes to GBS meningitis *in vivo*.** Groups of CD-1 mice (n = 9-10 per group) were injected intravenously with 1 x $10^9$ CFU COH1 WT or COH1Δ*mprF* mutant strains. Representative data from 2 independent experiments are shown (*n* = 20 for WT and *n* = 19 for Δ*mprF* mutant). Mice were sacrificed after 72 h and bacterial counts were assessed in the A) brain and B) blood. C) Histopathology of hematoxylin-eosin-stained brain sections from representative mice infected with COH1 WT (top panels) or COH1Δ*mprF* mutant (bottom panels), arrows indicate areas of meningeal thickening and leukocyte infiltration. D) Quantification of meningeal thickening using ImageJ. E) KC chemokine production in brain tissue was measured by ELISA. In panels A), B), D), and E) the bar indicates the Median. Statistical analyses: A), B), and D) unpaired two-tailed t-test, E) Mann-Whitney U test, p-values indicated.

**Table 1. Phospholipids and glycolipids present in strains used in this study[1].**

| Species | Strain | Lipids | | | | | | |
|---|---|---|---|---|---|---|---|---|
| | | PA | PG | CL | Lys-PG | Lys-Glc-DAG | MHDAG | DHDAG |
| GBS | COH1 | + | + | + | + | + | + | + |
| | A909 | + | + | + | + | + | + | + |
| | CNCTC 10/84 | + | + | + | + | + | + | + |
| | COH1Δ*mprF* | + | + | + | - | - | + | + |
| | COH1Δ*mprF*(pGBSMprF) | + | + | + | + | + | + | + |
| | COH1Δ*mprF*(pABG5Δ*phoZ*) | + | + | + | - | - | + | + |
| | COH1(pABG5Δ*phoZ*) | + | + | + | + | + | + | + |
| *S. mitis* | ATCC 49456(pABG5Δ*phoZ*) | + | + | + | - | - | + | + |
| | ATCC 49456(pGBSMprF) | + | + | + | + | + | + | + |
| | ATCC 49456(pEfmMprF1) | + | + | + | + | - | + | + |
| | ATCC 49456(pEfmMprF2) | + | + | + | - | - | + | + |

[1]Abbreviations: GBS, Group B *Streptococcus*; PA, phosphatidic acid; PG, phosphatidylglycerol; CL, cardiolipin; Lys-PG, lysyl-phosphatidylglycerol; Lys-Glc-DAG, lysyl-glucosyl-diacylglycerol; MHDAG, monohexosyldiacylglycerol; DHDAG, dihexosyldiacylglycerol.

**Table 2. Observed and calculated exact masses of the $[M+H]^+$ ions of Lys-Glc-DAG molecular species in *S. agalactiae* COH1.**

| Lys-Glc-DAG[1] | $[M+H]^+$ | |
|---|---|---|
| | Observed mass | Exact mass |
| C28:1 | 801.575 | 801.583 |
| C28:0 | 803.595 | 803.599 |
| C30:1 | 829.610 | 829.615 |
| C30:0 | 831.624 | 831.630 |
| C32:2 | 855.623 | 855.630 |
| C32:1 | 857.644 | 857.646 |
| C34:2 | 883.657 | 883.622 |
| C34:1 | 885.672 | 885.677 |
| C36:2 | 911.686 | 911.693 |
| C36:1 | 913.703 | 913.709 |

[1]The numbers before and after colons indicate the total acyl chain carbon atoms and double bonds, respectively.

**Supplementary Figures and Tables**

# *Streptococcus agalactiae* MprF synthesizes a novel cationic glycolipid that promotes brain entry and meningitis

Luke R. Joyce[1], Haider S. Manzer[2], Jéssica da C. Mendonça[2], Ricardo Villarreal[2], Kelly S. Doran[2#,] Kelli L. Palmer[1#], and Ziqiang Guan[3#]

[1]Department of Biological Sciences, The University of Texas at Dallas, Richardson, TX, USA

[2]Department of Immunology and Microbiology, University of Colorado School of Medicine, Aurora, CO, USA

[3]Department of Biochemistry, Duke University Medical Center, Durham, NC, USA

**Running title:** GBS lysine lipids contribute to meningitis

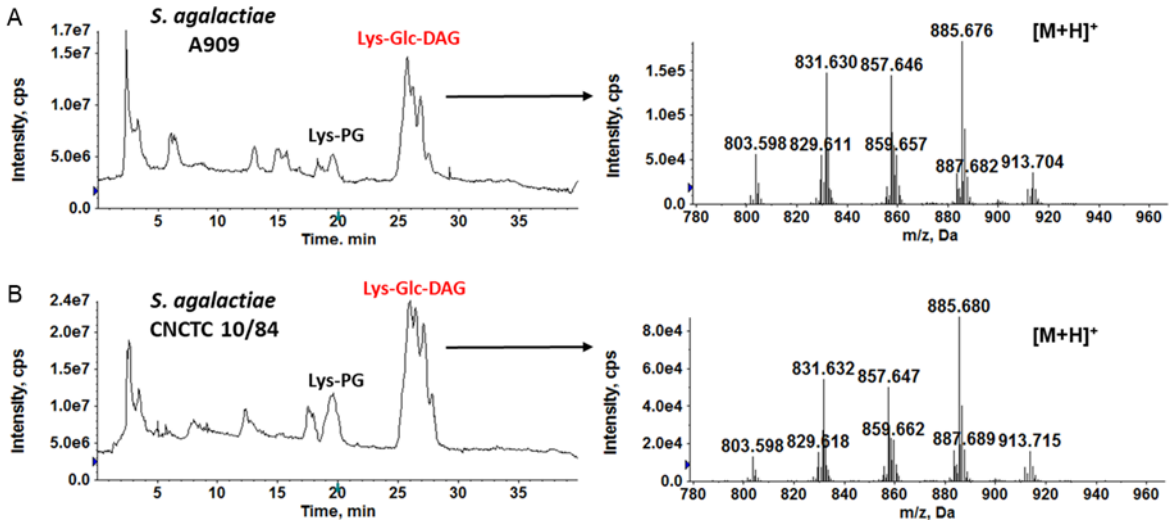


**Supplementary Figure 1. Detection of Lys-PG and Lys-Glc-DAG in *S. agalactiae* A909 and *S. agalactiae* CNCTC 10/84.** Positive TICs (left panels) showing the presence of Lys-PG and Lys-Glc-DAG in S. *agalactiae* A909 and S. *agalactiae* CNCTC 10/84. Mass spectra (right panels) show the $[M+H]^+$ ions of Lys-Glc-DAG.

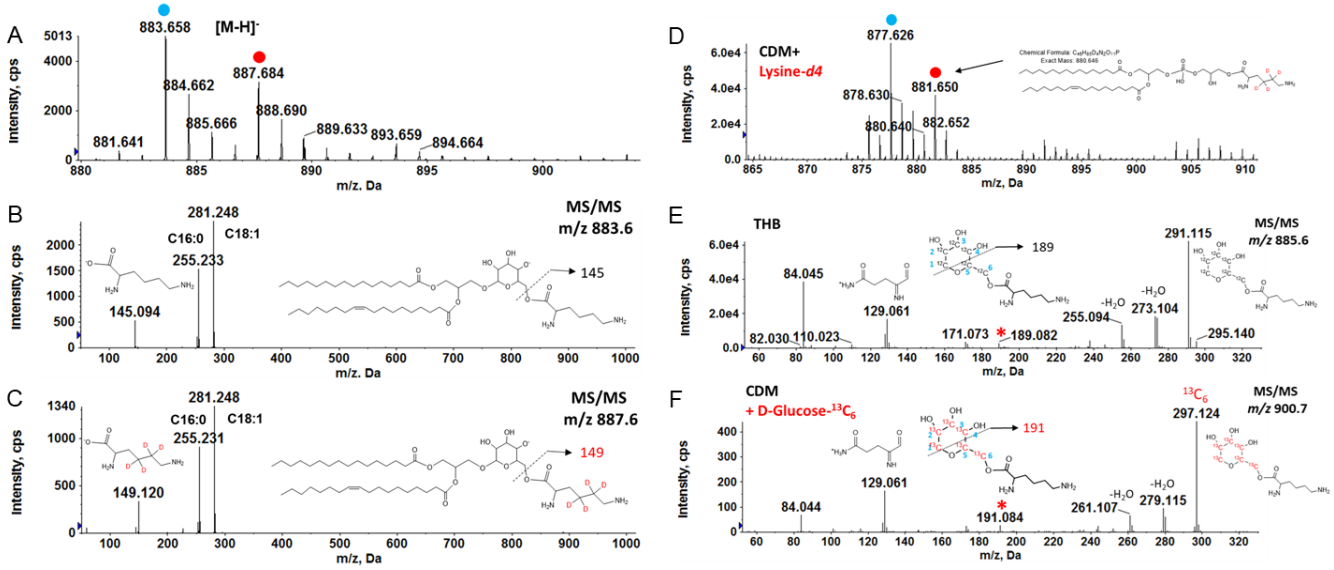


**Supplementary Figure 2. Isotopic incorporation of deuterated lysine and $^{13}$C-labeled glucose into Lys-Glc-DAG and Lys-PG.** The lipid extracts of *S. agalactiae* COH1 cultured in DM, DM supplemented with 450 µM L-lysine-*d4* (4,4,5,5-D4), or in DM containing 0.5% w/v D-Glucose (U-$^{13}C_6$) were analyzed by LC-ESI/MS in the positive ion mode. A) Negative ESI/MS of $[M-H]^-$ ions of major Lys-Glc-DAG species in *S. agalactiae* COH1 when cultured in DM supplemented with lysine-*d4*. The incorporation of lysine-*d4* into Lys-Glc-DAG is evidenced by an upward *m/z* shift of 4 Da of the $[M-H]^-$ ion (from *m/z* 883 to *m/z* 887). B) MS/MS of $[M-H]^-$ at *m/z* 883.6 produces a deprotonated lysine residue at *m/z* 145. C) MS/MS of $[M-H]^-$ at *m/z* 887.6 produces a deprotonated lysine-*d4* residue at *m/z* 149. D) $[M+H]^+$ ions of major Lys-PG species in *S. agalactiae* COH1 cultured in DM supplemented with lysine-*d4.* The incorporation of lysine-*d4* in Lys-PG is evidenced by an upward *m/z* shift of 4 Da from unlabeled Lys-PG (blue dot) to labeled Lys-PG (red dot). E) MS/MS of 885.6. A major product ion at *m/z* 291.1 is derived from glucose-lysine residue. F) MS/MS of *m/z* 900.7 (containing fifteen $^{13}$C atoms). The presence of *m/z* 297.1 (with 6 Da shift) is consistent with glucose in Lys-Glc-DAG is replaced with D-Glucose (U-$^{13}C_6$). The other nine $^{13}$C atoms are incorporated into the DAG portion of Lys-Glc-DAG. Furthermore, MS/MS data indicate that lysine is linked to the C6 position of glucose by the fragmentation schemes for forming *m/z* 189 ion from the unlabeled Lys-Glc-DAG and *m/z* 191 ion from the $^{13}$C-labeled Lys-Glc-DAG.

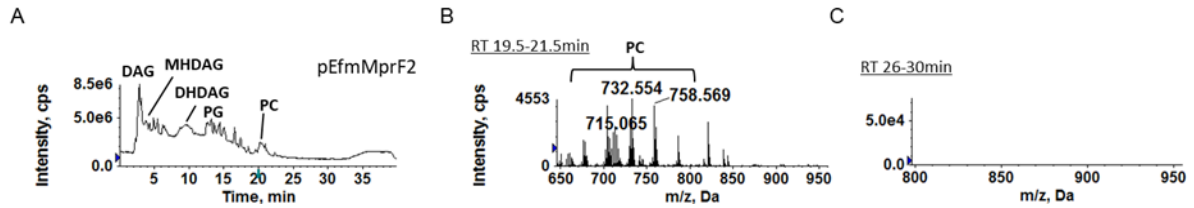


**Supplementary Figure 3. Neither Lys-PG nor Lys-Glc-DAG is produced by *E. faecium* MprF2 expression in *S. mitis*.** The lipid extracts of *S. mitis* (ATCC 49456) cells expressing *E. faecium mprF2* (pEfmMprF2) was analyzed by LC-ESI/MS in the positive ion mode. A) TIC of 49456(pEfmMprF2) shows the whole lipidomic profile. B) MS of retention time 19.5 – 21.5 min showing the absence of Lys-PG in the strain. C) MS of retention time 26 – 30 min showing the absence of Lys-Glc-DAG. This data is consistent with a previous report that the *mprF2* allele in the *E. faecium* genome is inactive (1).

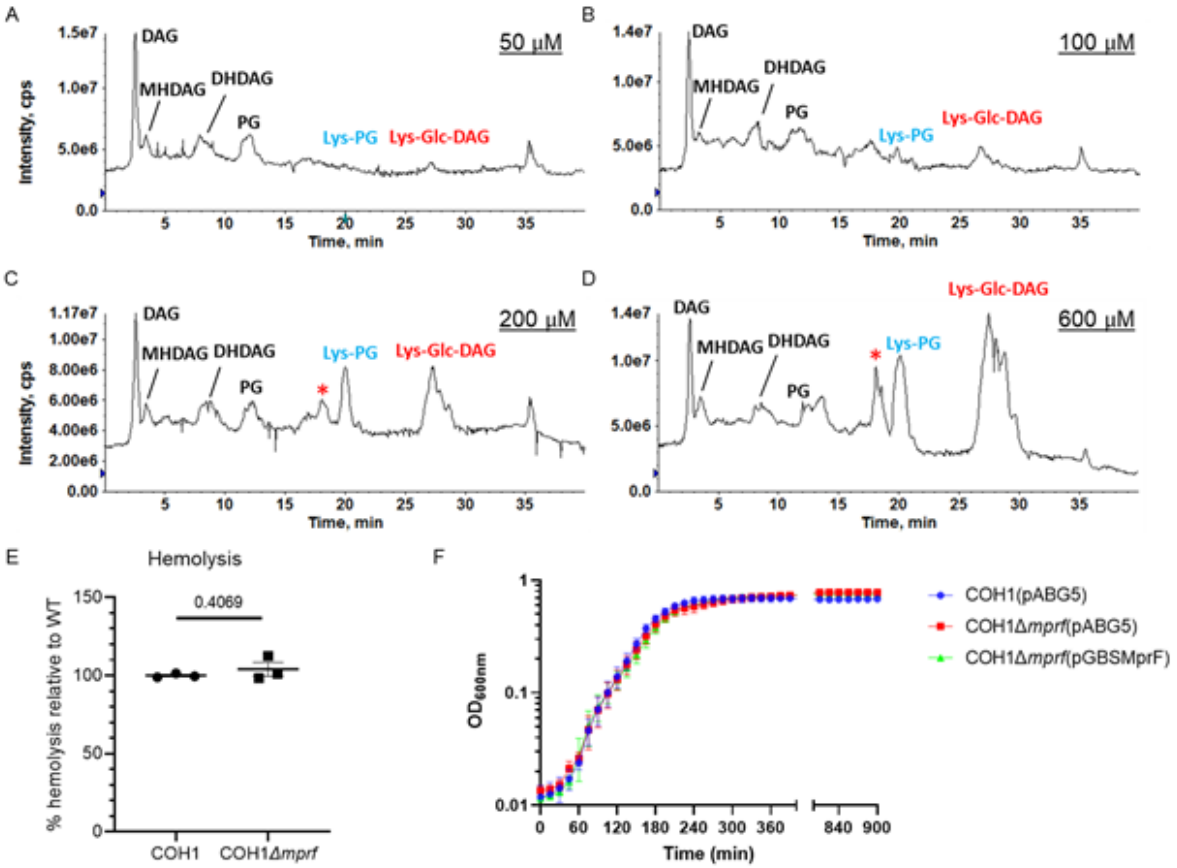


**Supplementary Figure 4. Lysine titration TICs and absence of hemolytic and growth phenotypes of COH1Δ*mprF* mutant.** Shown are positive TICs of LC-ESI/MS of lipid extracts of COH1 cultured in defined growth media containing A) 50 µM lysine, B) 100 µM lysine, C) 200 µM lysine and D) 600 µM lysine. Lys-Glc-DAG and Lys-PG levels in COH1 positively correlate with lysine concentration in the growth medium. "*" denotes methylcarbamate, an extraction artifact of Lys-Glc-DAG. E) Hemolytic activity of WT COH1 and Δ*mprF* mutant. Mean and SEM indicated, statistical analysis: unpaired two-tailed t-test, p-value indicated. F) Growth curves of COH1(pABG5) (blue), COH1Δ*mprF*(pABG5) (red), and COH1Δ*mprF*(pGBSMprF) (green). There is no observable growth defect under these conditions. Mean and SD indicated.

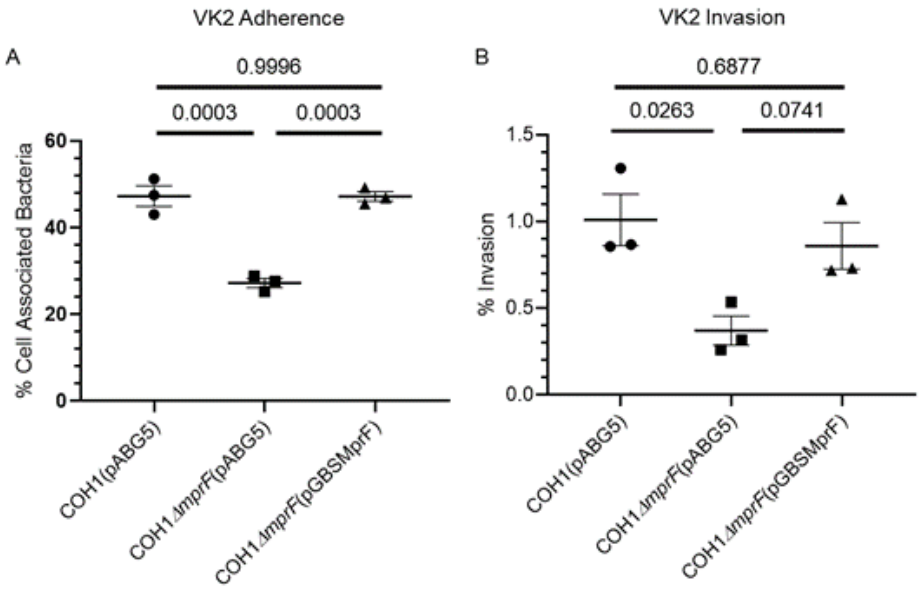


**Supplementary Figure 5. MprF contributes to GBS adhesion and invasion of a human epithelial cell line *in vitro*.** COH1(pABG5), Δ*mprF*(pABG5), and complement strain Δ*mprF*(pGBSMprF) were tested for A) adhesion and B) invasion of the vaginal epithelial VK2/E6E7 cell line. The Δ*mprF*(pABG5) strain displays a significant decrease in both adhesion and invasion compared to WT and complement strains. *In vitro* tissue culture assay results are the mean of three replicate experiments, each with four technical replicates. Mean and SEM indicated, statistical analyses: One-way ANOVA with Tukey's multiple comparisons test, p-values indicated on figures.

**Supplementary Table 1. Strains and plasmids used in this study.**

| Organism | Strain | Description | Ref |
|---|---|---|---|
| *S. agalactiae* | ATCC BAA-1176 (COH1) | Wild-type *S. agalactiae* strain, serotype III | (2) |
| | COH1Δ*mprF* | *mprF* (GBSCOH1_1931) deletion strain | This work |
| | COH1Δ*mprF(*pABG5) | Empty vector control strain | This work |
| | COH1Δ*mprF*(pGBSMprf) | Expresses GBS *mprF* from $P_{prtF}$ in pABG5Δ*phoZ* | This work |
| | COH1(pABG5) | Empty vector control | This work |
| | ATCC BAA-1138 (A909) | Wild-type *S. agalactiae* strain, serotype Ia | (3) |
| | CNCTC 10/84 | Wild-type *S. agalactiae* strain, serotype V. Obtained from Dr. K Patras, UCSD | (4,5) |
| *S. mitis* | ATCC 49456 | Wild-type *S. mitis* type strain, also known as NCTC 12261 | (6) |
| | ATCC 49456(pABG5) | Empty vector control | This work |
| | ATCC 49456(pGBSMprF) | Expresses GBS *mprF* from $P_{prtF}$ in pABG5Δ*phoZ* | This work |
| | ATCC 49456(pEfmMprF1) | Expresses *E. faecium mprF1* from $P_{prtF}$ in pABG5Δ*phoZ* | This work |
| | ATCC 49456(pEfmMprF2) | Expresses *E. faecium mprF1* from $P_{prtF}$ in pABG5Δ*phoZ* | This work |
| *E. coli* | DH5α | Plasmid cloning host; $F^-$, φ80*lac*ZΔM15, *rec*A1, *end*A1, *hsd*R17, *pho*A, *sup*E44, $\lambda^-$ *thi*-1, *gyr*A96, *rel*A1 | (7) |
| | DH5α(pABG5) | Empty vector control | This work |
| | DH5α(pGBSMprF) | Expresses COH1 *mprF* (GBSCOH1_1931) from $P_{prtF}$ in pABG5Δ*phoZ* | This work |
| | DH5α(pEfmMprF1) | Expresses *E. faecium mprF1* from $P_{prtF}$ in pABG5Δ*phoZ* | This work |
| | DH5α(pEfmMprF2) | Expresses *E. faecium mprF1* from $P_{prtF}$ in pABG5Δ*phoZ* | This work |
| | DH5α(pMBMprFKO) | Allelic exchange plasmid containing ~2 kb sequence flanking GBSCOH1_1931 | This work |
| *E. faecium* | 1,231,410 | Wild type *E. faecium* strain | (8) |

| Plasmid | Description | Ref |
|---|---|---|
| pABG5Δ*phoZ* | Constitutive expression vector for streptococci with the $P_{prtF}$ promoter. Confers kanamycin resistance. Referred to as pABG5 throughout the text | (9) |
| pGBSMprF | pABG5Δ*phoZ* expressing COH1 *mprF* (GBSCOH1_1931) from $P_{prtF}$ | This work |

| | | |
|---|---|---|
| pEfmMprF1 | pABG5Δ*phoZ* expressing *E. faecium* 1,231,410 *mprF1* (EFTG_00601) from $P_{prtF}$ | This work |
| pEfmMprF2 | pABG5Δ*phoZ* expressing *E. faecium* 1,231,410 *mprF2* (EFTG_02430) from $P_{prtF}$ | This work |
| pMBSacB | Allelic exchange plasmid for *S. agalactiae*. Confers erythromycin resistance and sucrose sensitivity | (10) |
| pMBMprFKO | Knockout plasmid containing ~2 kb sequence flanking GBSCOH1_1931 | This work |

## Supplementary Table 2. Primers used in this study.

| Primer | 5' – 3' sequence | Use |
|---|---|---|
| GBS_MprF_F | GAGAGGTCCCTTTCCTTGAAAAAGCTAATTGAAAAAGTC | Amplify GBSCOH1_1931 for Gibson assembly |
| GBS_MprF_R | ACCAATACCTTTATCTTATTTAACAATCTTAATTTTACTATC | Amplify GBSCOH1_1931 for Gibson assembly |
| Faec_MprF1_F | GAGAGGTCCCTTTCCTTGTTAAAAAATACCATACAATG | Amplify EFTG_00601 for Gibson assembly |
| Faec_MprF1_R | ACCAATACCTTTATCTTAATACTTTCTTCGTATCC | Amplify EFTG_00601 for Gibson assembly |
| Faec_MprF2_F | GAGAGGTCCCTTTCCGTGAAAAATAAACGATACTTG | Amplify EFTG_02430 for Gibson assembly |
| Faec_MprF2_R | ACCAATACCTTTATCTTATAATTCTGTGAGCACTTC | Amplify EFTG_02430 for Gibson assembly |
| pABG5-5' | GGAAAGGGACCTCTCTTCCTAAAC | Linearize pABG5Δ*phoZ* for Gibson assembly |
| pABG5-3' | GATAAAGGTATTGGTAAATAACAAA | Linearize pABG5Δ*phoZ* for Gibson assembly |
| | **Expression plasmid sequencing** | |
| GBS_S1 | GAATGGAATAATATAGTAGGCT | For sequencing pGBSMprF, amplifies with pABG5_Fup2 |
| GBS_S2 | GATTGTATCCCTTATTCC | For sequencing pGBSMprF, amplifies with GBS_S3 |
| GBS_S3 | CGATTCAATAGCTTCAC | For sequencing pGBSMprF, amplifies with GBS_S2 |
| GBS_S4 | GATAAAAGGCTCTACTGG | For sequencing pGBSMprF, amplifies with pABG5_FDwn |
| pABG5_FDwn | CCAATAATAATGACTAGAGAAG | For pABG5 plasmid insert sequencing |
| pABG5_Fup2 | CAAAAGGTTTCGACTTTTCACC | For pABG5 plasmid insert sequencing |
| EF1_S1 | GAATAACGCTGATCAAAAGT | For sequencing pEfmMprF1, amplifies with pABG5_Fup2 |
| EF1_S2 | TGCCAAGAGAAATAGTC | For sequencing pEfmMprF1, amplifies with EF1_S3 |
| EF1_S3 | ACAATCTCTTCGCTTG | For sequencing pEfmMprF1, amplifies with EF1_S2 |
| EF1_S4 | CCAACTGTTCTTCTCCAA | For sequencing pEfmMprF1, amplifies with pABG5_FDwn |
| EF2_S1 | CTCCTGTATGTGTGATGAAC | For sequencing pEfmMprF2, amplifies with pABG5_Fup2 |
| EF2_S2 | GGAATGGGGACTTTTGA | For sequencing pEfmMprF2, amplifies with EF2_S3 |
| EF2_S3 | ACTGATTCGTTGCTGC | For sequencing pEfmMprF2, amplifies with EF2_S2 |
| EF2_S4 | CTTCGCTTGTCAGGTTAC | For sequencing pEfmMprF2, amplifies with pABG5_FDwn |
| **GBSCOH1_1931 knockout plasmid construction, sequencing, and integration screening** | | |
| Mp1F_PstI | ACGTCACTGCAGTTCAATTAGCTTTTTCAACAATTTC | Amplifies upstream fragment from within GBSCOH1_1931 leaving 6 codons, with Mp1R_XhoI |
| Mp1R_XhoI | ACGTCACTCGAGGCTGTTTATGGTGCTTTG | 5' most primer of upstream fragment, amplifies with Mp1F_PstI |
| Mp2F_XbaI | ACGTCATCTAGAGAAAAGGCTAGATTACGAAC | 3' most primer of downstream fragment, amplifies with Mp2R_PstI |
| Mp2R_PstI | ACGTCACTGCAGGTTAAATAAGCTTTATTTGGCA | Amplifies downstream fragment leaving 2 codons and stop codon of GBSCOH1_1931, with Mp2F_XbaI |
| T7 promoter | TAATACGACTCACTATAGGG | Amplifies with MpS5F below to sequence plasmid, amplifies with T3 promoter for insert screening and plasmid presence |
| T3 promoter | AATTAACCCTCACTAAAGGG | Amplifies with MpS3R below, amplifies with T7 promoter for insert screening and plasmid presence |

| | | |
|---|---|---|
| Int_F | GCTAATTGAACTGCAGGTTAAATAAG | Anneals at *mprF* knockout site, amplifies with Out_R for single integration screening |
| Out_R | GCTATTATATTTAGTGGTTTAATTGG | Anneals outside recombination arms, amplifies with Int_F, for single integration screening |
| | **Genomic knockout region sequencing** | |
| MpS3F | CATTAGCTAGTCTTATCGGAG | Anneals outside integration arms, amplifies with MpS3R |
| MpS3R | ACAGCTACTTGGTAGTTCA | Amplifies with MpS3F |
| MpS4F | GCTACTAAGGCAAGATACG | Amplifies with MpS4R, knockout screening and plasmid sequencing primer |
| MpS4R | ATGGTCAGCGATGGTG | Amplifies with MpS4F, knockout screening and plasmid sequencing primer |
| MpS5F | CATAAGCGAAATAACTTGAG | Amplifies with MpS5R |
| MpS5R | GTATACAACGGCTTGATTGG | Anneals outside integration arms, amplifies with MpS5F |

## References


1. Roy H, Ibba M. Broad range amino acid specificity of RNA-dependent lipid remodeling by multiple peptide resistance factors. *J Biol Chem*. 2009;284(43):29677-29683.

2. Kuypers JM, Heggen LM, Rubens CE. Molecular analysis of a region of the Group B Streptococcus chromosome involved in type III capsule expression. *Infect Immun*. 1989;57(10):3058-3065.

3. Lancefield RC, McCarty M, Everly WN. Multiple mouse-protective antibodies directed against group B streptococci. Special reference to antibodies effective against protein antigens. *J Exp Med*. 1975;142(1):165-179.

4. Wilkinson HW. Nontypable group B streptococci isolated from human sources. *J Clin Microbiol*. 1977;6(2):183-184.

5. Hooven TA, et al. Complete Genome Sequence of *Streptococcus agalactiae* CNCTC 10/84, a Hypervirulent Sequence Type 26 Strain. *Genome Announc*. 2014;2(6).

6. Kilian M, Mikkelsen L, Henrichsen J. Taxonomic Study of Viridans Streptococci: Description of *Streptococcus gordonii* sp. nov. and Emended Descriptions of *Streptococcus sanguis* (White and Niven 1946), *Streptococcus oralis* (Bridge and Sneath 1982), and *Streptococcus mitis* (Andrewes and Horder 1906). *Int J Syst Bacteriol*. 1989;39(4):471-484.

7. Taylor RG, Walker DC, McInnes RR. *E. coli* host strains significantly affect the quality of small scale plasmid DNA preparations used for sequencing. *Nucleic Acids Res*. 1993;21(7):1677-1678.

8. Palmer KL, et al. High-quality draft genome sequences of 28 *Enterococcus* sp. isolates. *J Bacteriol*. 2010;192(9):2469-2470.

9. Granok AB, Parsonage D, Ross RP, Caparon MG. The RofA binding site in *Streptococcus pyogenes* is utilized in multiple transcriptional pathways. *J Bacteriol*. 2000;182(6):1529-1540.

10. Hooven TA, Bonakdar M, Chamby AB, Ratner AJ. A Counterselectable Sucrose Sensitivity Marker Permits Efficient and Flexible Mutagenesis in *Streptococcus agalactiae*. *Appl Environ Microbiol*. 2019;85(7):1-13.